5.4 Industry Standard Nondestructive Evaluations

Comment [PGO39]: We will talk further about this on the phone.

Standard ultrasonic evaluation techniques used by in-service inspection (ISI) vendors include time-of-flight diffraction (TOFD) for detecting cracks in both the circumferential and axial orientation and zero-degree pulse echo for an interference fit examination. Blade probes (low profile) and solid-probe head configurations are deployed depending on the access conditions of the CRDM assembly (EPRI 2005; IAEA 2007, and discussions with JP Lareau, WesDyne International). An examination conducted by ISI vendor, WesDyne International (data supplied by JP Lareau), discovered a probable leak path in Nozzle 63. The data acquired with industry-standard 5.0-and 2.25-MHz probes are shown in Figures 5.17 and 5.18, respectively. The 2.25-MHz image in Figure 5.18 has a lower resolution than the 5.0-MHz image in Figure 5.17 as expected, but both data sets detect the leak path observed at the low point (industry's zero-degree position) of the interference fit region.

Comment [PGO40]: What is the context for this examination? Was this done while the head was still on or after it was replaced?

The Figure 5.17 image can be compared to the PNNL's results in Figure 5.15. Both data sets were acquired with probes having nominal center frequencies of 5 MHz and they show the main leak path as a high-amplitude signal. In the WesDyne data, this is represented by the magenta color. Both data images capture other partial leak paths and show similar areas of high and low reflectivity. The PNNL data however possess better data registration in the odd and even scan lines as well as improved resolution and focusing. These images demonstrate that PNNL was successful in achieving a better evaluation of the interference fit as compared to a qualified industry procedure.

Comment [PGO41]: Remove this.

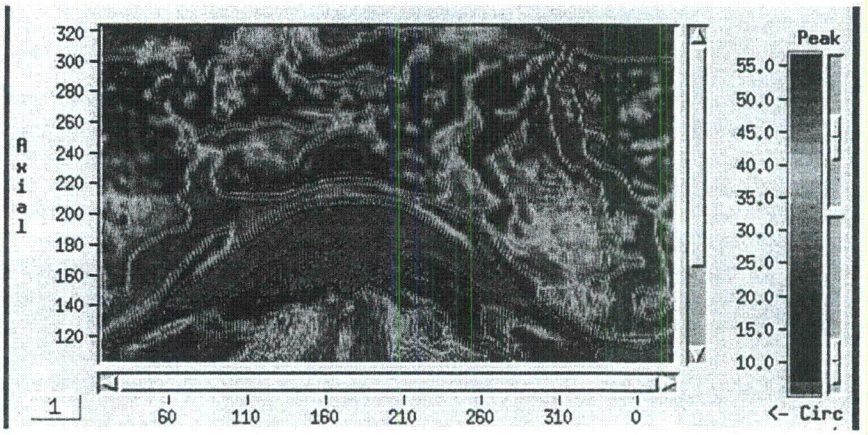

Figure 5.17 Ultrasonic Data from Nozzle 63 as Obtained by WesDyne International. The image was acquired with a 5-MHz probe. The horizontal axis represents the nozzle circumference in units of degrees. The vertical axis represents the nozzle axis in units of millimeters.

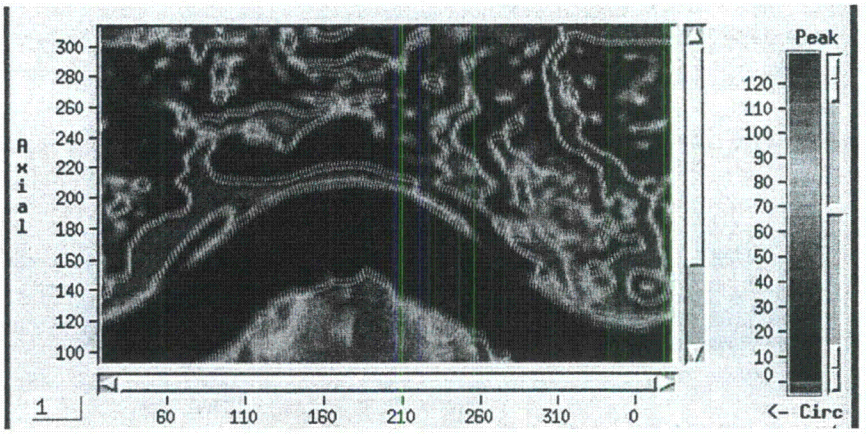

Figure 5.18 Ultrasonic Data from Nozzle 63 as Obtained by WesDyne International. The image was acquired with a 2.25-MHz probe. The horizontal axis represents the nozzle circumference in units of degrees. The vertical axis represents the nozzle axis in units of millimeters.

Additionally, an eddy current inspection conducted by WesDyne International detected two axial flaws. These were found at the locations shown in Figure 5.19 (data supplied by JP Lareau). The specific circumferential locations were noted at 172 and 360 degrees with 0 or 360 degrees representing the downhill position. The axial length for flaw 1, below the weld, was 25.4 mm (1.0 in.) and for flaw 2, above the weld and in the main leak path, was 19.3 mm (0.76 in.). These cracks were ID surface-connected and reported as shallow flaws.

While PNNL did not specifically perform an evaluation for axial cracking in the Alloy 600 tube, the two axial cracks noted by industry were detected. The zero-degree PNNL inspection was not optimized for crack detection as an axial crack presented only a knife-edge profile to the ultrasonic beam and did not reflect much energy. Nevertheless, the cracks were visible in the interference fit response and on further analysis also marginally detected in the water-to-Alloy 600 tube reflection (ID surface of the tube). Figure 5.20 shows the uphill images for the ID tube and interference fit responses. Similarly Figure 5.21 shows the responses for the downhill images. Both flaws appear to be ID surface-connected as they were detected in the data acquired at the ID surface of the Alloy 600 tube. These two flaws are also evident in the image in Figure 5.15. The ultrasonic data did not provide any depth-sizing information.

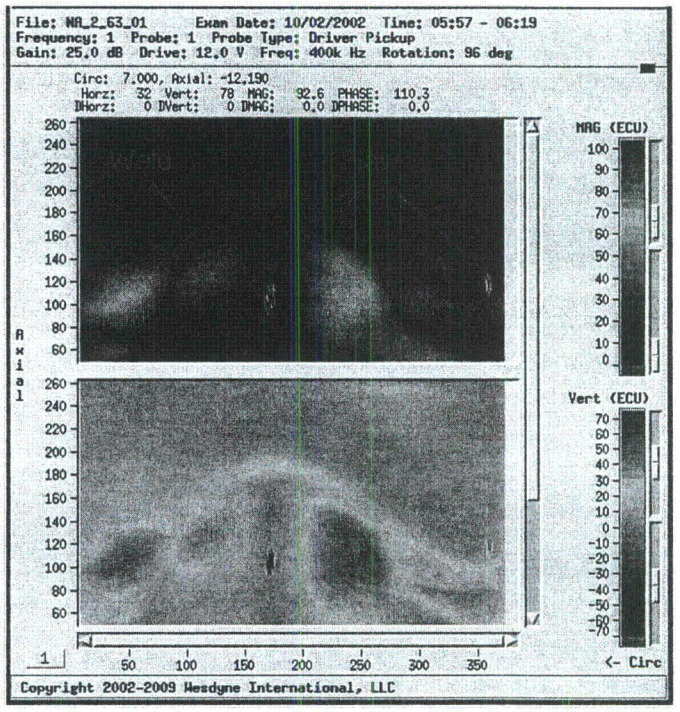

Figure 5.19 Eddy Current Data (WesDyne International) Showing Two Axial Flaws. The horizontal axis represents the nozzle circumference in degrees. The vertical axis represents the nozzle axis in millimeters.

Comment [PGO42]: What is the difference between the top and bottom image?

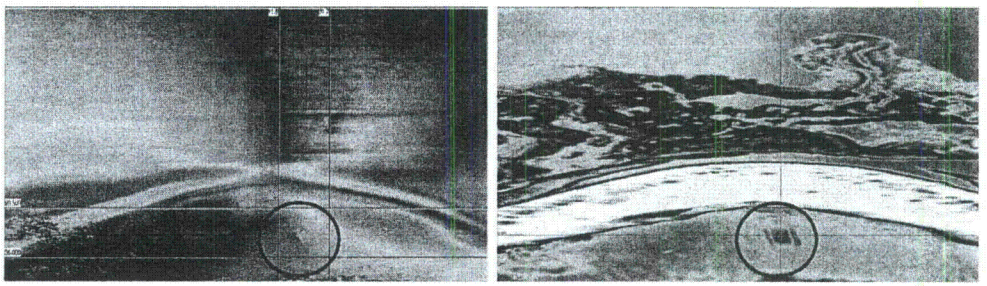

Figure 5.20 Uphill Nozzle ID Response on the Left and Interference Fit Response on the Right with the Axial Flaw Indication Circled. The horizontal axes represent 189 degrees and the vertical axes represent 360 mm (14.2 in.).

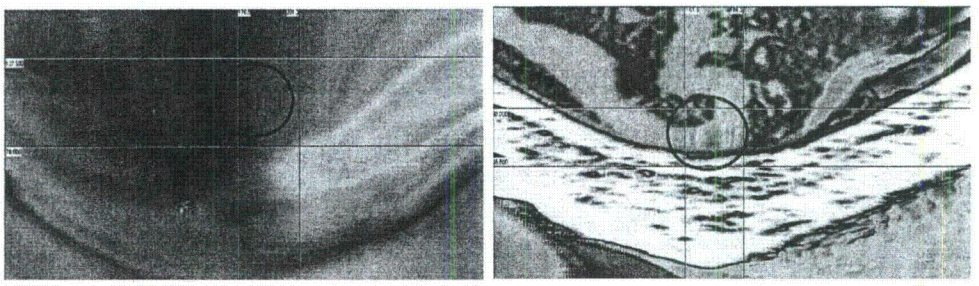

Figure 5.21 Downhill Nozzle ID Response on the Left and Interference Fit Response on the Right with the Axial Flaw Indication Circled. The horizontal axes represent 188 degrees and the vertical axes represent 155 mm (6.1 in.).

Comment [PGO43]: All discussion of eddy current flaw analysis should be removed.

6 Destructive Validation of Nozzle 63

Confirmatory destructive testing was necessary on Nozzle 63 to validate the ultrasonic characterizations of the leak path(s) and other areas of interest as described in Section 5. The destructive testing activity was conducted by Babcock and Wilcox Technical Services Group (B&W) located at the Lynchburg, Virginia, facility. This activity required the dismantling of the interference fit region with full separation of the Alloy 600 tube from the reactor vessel head (RVH) material to reveal true-state information with regard to the leak path(s), boric acid deposit regions, and wastage regions. Pacific Northwest National Laboratory (PNNL) personnel were on site during the critical sectioning activities to identify proper cutting locations. Additionally, the J-groove weld region was preserved and returned to PNNL for storage in anticipation of future work.

B&W used an industrial 19-ft CobraFab Industries, Inc. band saw model VH2532HD with 'Cobra Strike' and an interchangeable blade option for all cutting purposes associated with the destructive activity. This saw was equipped with a ±45° hydraulic miter attachment and was capable of cutting pieces measuring 63.5 cm (25 in.) wide by 81.3 cm (32 in.) high in the vertical position and 63.5 cm (25 in.) wide by 55.9 cm (22 in.) high in the ±45° positions. A total of six 5.8 m (19-ft) blades were acquired from Scarney Industries, Youngstown, Ohio. Two coarse tooth (2-3 teeth per inch) and three fine tooth (4-6 teeth per inch) bimetallic blades with positive rake, variable pitch, and variable tooth were used. Additionally, one carbide grit-abrasive blade was also used. In general, coarse tooth blades were used for thicker section cutting, 20.3 cm (8 in.) and larger, and the fine toothed blades were used for precision cutting material under 20.3 cm (8 in.) in thickness. The carbide grit abrasive blade was used when the bimetallic blades were ineffective. Figure 6.1 shows the three blade types used. All cuts in this activity were conducted without lubrication or coolant to minimize disturbance to the interference fit region.

Comment [PGO44]: Section on cutting can be substantially shortened. Only need a few pictures and paragraphs to describe what we did: 1 paragraph/figure on size reduction cut, 1 paragraph/figure on bisection cut, 1 paragraph/figure on weld removal cut.

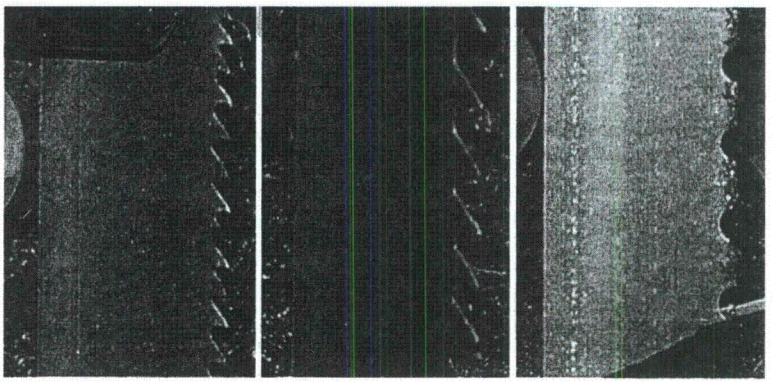

Figure 6.1 **Three Blade Types were Utilized to Section the RPV Head and CRDM Nozzle. From left: fine tooth blade, coarse tooth blade, and carbide grit blade.**

Comment [PGO45]: Remove this figure.

The initial size reduction cuts were performed on the Nozzle 63 specimen using one of the coarse toothed blades prior to the arrival of PNNL staff. Non-essential material was removed to reduce weight and to facilitate proper blade placement on the specimen during critical cuts. Figure 6.2 shows images from the size reduction activity.

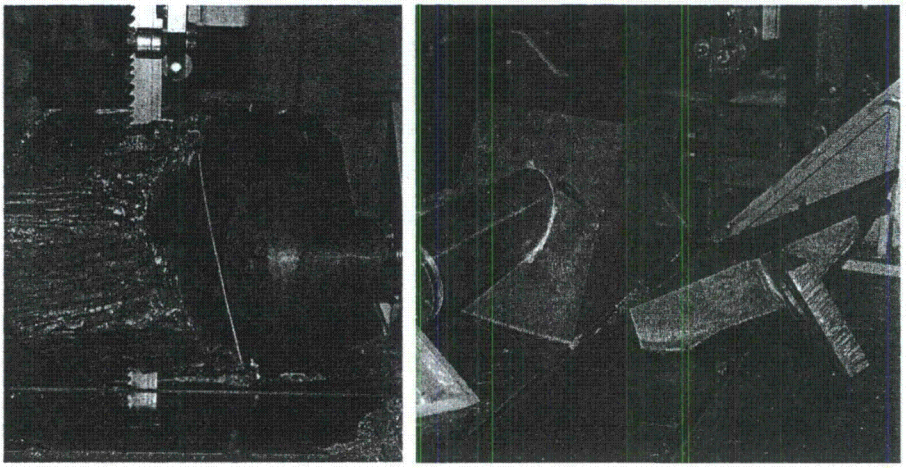

Figure 6.2 Size Reduction Cutting Activity

Comment [PGO46]: Can keep this figure.

After size reduction, the nozzle assembly was prepared for the dissection cut that separated the high and low sides of the assembly. The cut line was selected to start at approximately the 95-degree mark (Figure 6.3), and follow through to the 275-degree mark. The line placement was based on the ultrasonic data and chosen to preserve the primary leak path previously identified in the ultrasonic images.

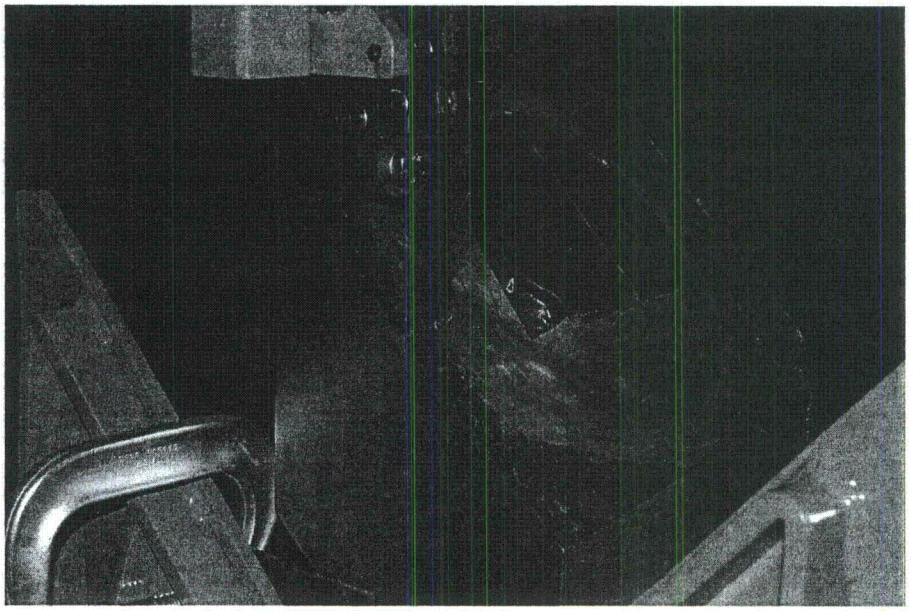

Figure 6.3 Start of the Dissection Cut

Comment [PGO47]: Keep this figure.

Dissection cutting began with the coarse-toothed blade. The cut progressed for approximately 20 minutes until an unidentified 'hard spot' was reached at the outer edge of the Alloy 600 nozzle region and stopped the cutting progression. A slower feed rate with a faster blade speed was attempted, but did not traverse the hard spot. The cause of the hard spot was not fully investigated, but a likely cause was from a cold-worked region of material within the heat-affected zone of the J grove weld adjacent to the nozzle outer diameter (OD). The coarse-cut blade was exchanged with a fine-toothed cutting blade and the cut was attempted again without success. Finally, the carbide blade was employed to abrasively grind through the hard spot. This blade required a greatly reduced feed rate, thus lengthened the cutting time. Further, the kerf of the carbide blade was thicker than the cutting blades, requiring the cut to be restarted at the initial cut path. The carbide grit abrasive blade is shown in Figure 6.4. The cut through this hard spot required approximately 2 hours to complete.

Comment [PGO48]: What is this term?

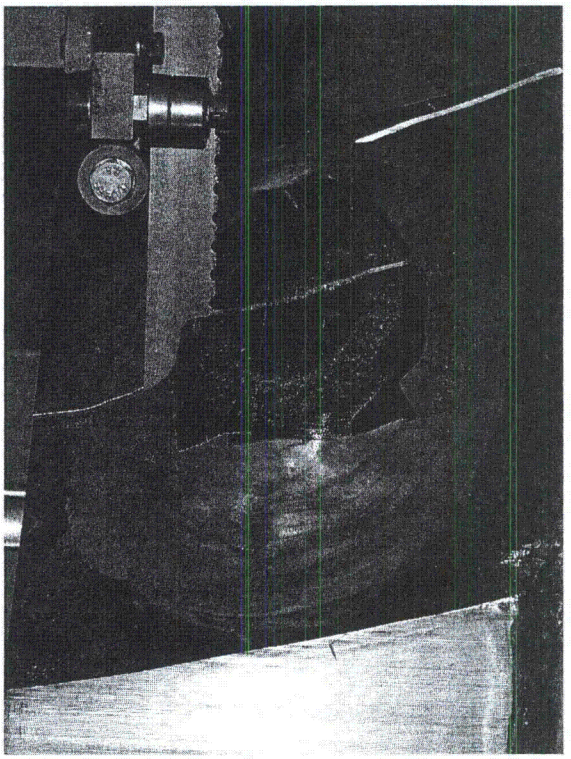

Figure 6.4 Abrasive Carbide Blade Progressing Through the Hard Spot

Comment [PGO49]: Remove this figure.

After cutting through the first side of the nozzle, the carbide blade was exchanged with the fine-toothed cutting blade and the dissection cutting continued. Another hard spot was incurred in the J-groove weld region. Again, the carbide blade was used to cut through the hard spot with a slow feed rate. Finally, the fine-toothed blade was re-engaged and the dissection cut completed. From the exposed surfaces, the triple point was identified along with the weld and butter regions as shown in Figure 6.5.

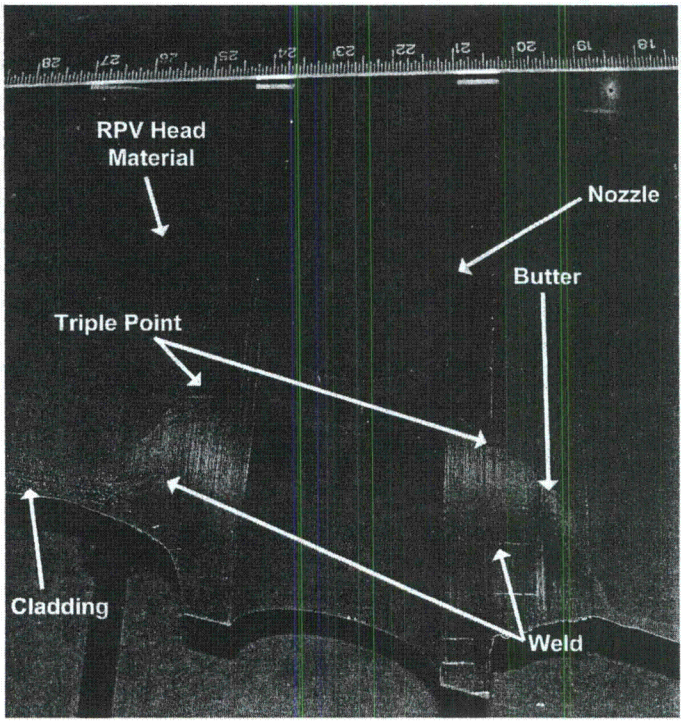

Figure 6.5 Nozzle 63 Assembly Cut in Half by Dissection Cut

Comment [PGO50]: Keep this figure. Remove all labels except RPV head and weld. Draw a line on this figure to show where the weld removal cut was made.

The cut to remove the J-groove weld was made 6.35 mm (0.25 in.) above the butter/triple point region in the reactor pressure vessel (RPV) head as seen in Figure 6.6. The high or uphill side half-portion was selected for the first cutting. As previously stated, the 'high' side has several potential leak paths whereas the 'low' or downhill side had the primary leak path as identified in the ultrasonic data. The specimen was secured and the band saw tilted to an approximate 43-degree angle to match the angle between the nozzle and head as shown in Figure 6.7. Cutting at this angle maximized the annulus region that was exposed while keeping the weld and butter regions intact for future evaluation. As the cut was designed to pass only through the low-alloy RVH material, the fine toothed cutting blade was selected for use. During the J-groove weld removal cut, another hard spot was encountered near the outside of the nozzle. Attempts were made to continue cutting with the fine-toothed blade until abrasive wear on one side of the blade resulted in the cut veering away from the desired cut line. Blades were exchanged and the carbide blade was used to cut through the hard spot and also to finish the cut. Before the cut broke through the inside of the tube, a vacuum equipped with a high-efficiency particulate air (HEPA) filter was added to collect and capture any radioactive oxide particles that were discharged from the cut as pictured in Figure 6.8.

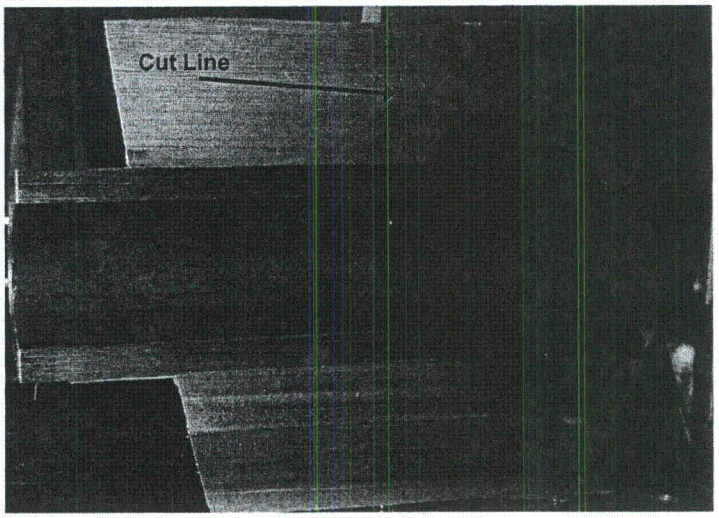

Figure 6.6 J-groove Weld Removal Cut Line Placement

Comment [PGO51]: Remove this figure.

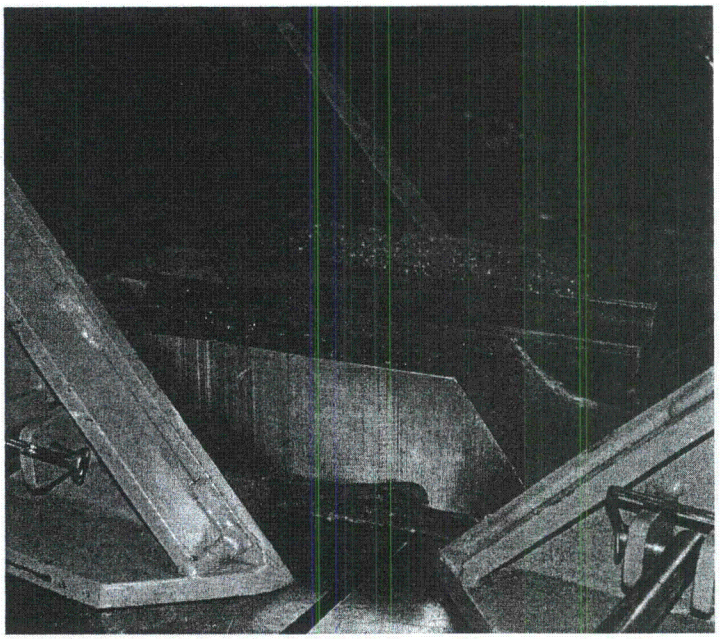

Figure 6.7 J-groove Weld Cut on the High Side

Comment [PGO52]: Remove this figure.

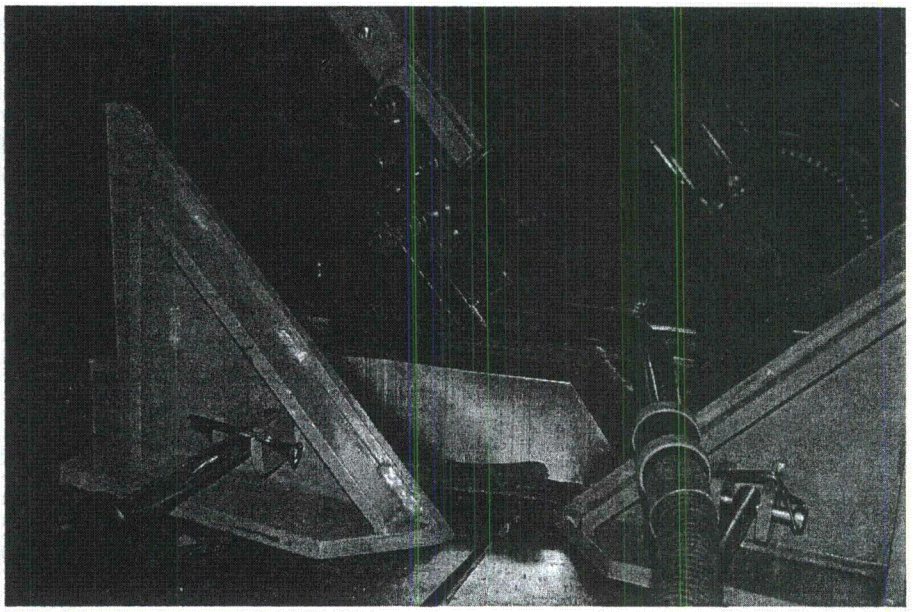

Figure 6.8 Abrasive Blade Cutting Through the Nozzle with a HEPA Vacuum Nozzle

Comment [PG053]: Remove this figure.

The cutting continued until the entire nozzle was separated from the J-groove weld region as pictured in Figure 6.9. At this point, the nozzle region above the weld was freely released from the RPV head material. Removal of the nozzle exposed the annulus region of the high-side section as shown in Figure 6.10. At this point all available blades were exhausted. Replacement blades were ordered to finish the cut and complete removal of the J-groove weld region. A Nikon D40x camera was used to acquire high-resolution photographic documentation of the annulus region. This activity was provided by B&W. A subsequent cut was conducted on the low-side section to expose its annulus region containing the primary leak path (Figure 6.11). The nozzle freely released from this portion as well.

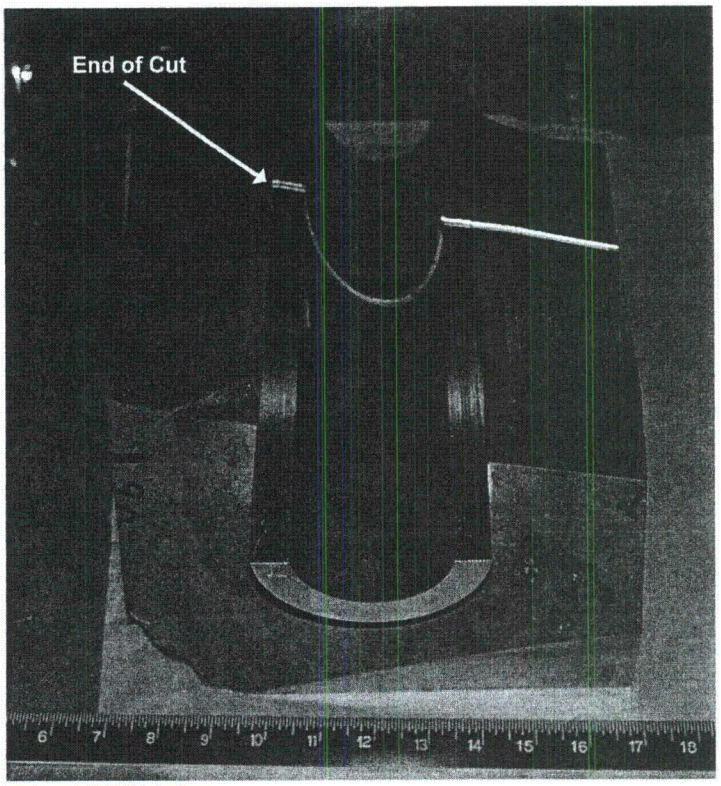

Figure 6.9 End of J-groove Weld Removal Cut

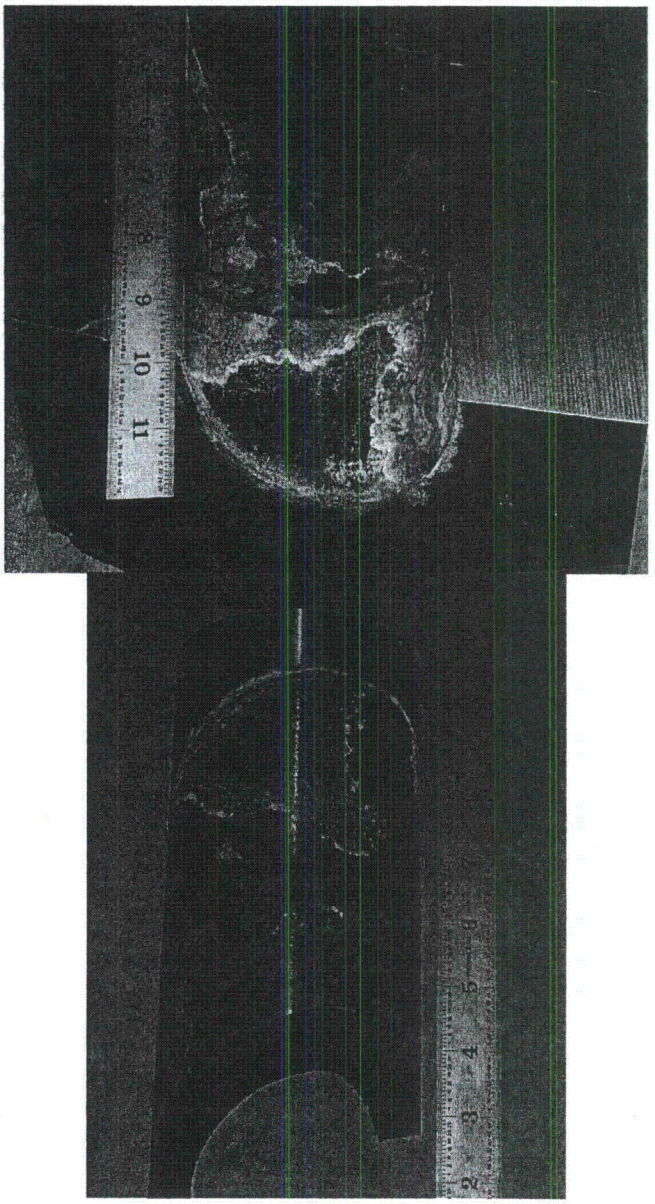

Figure 6.10 Exposed RPV Head and Nozzle from High Side Section

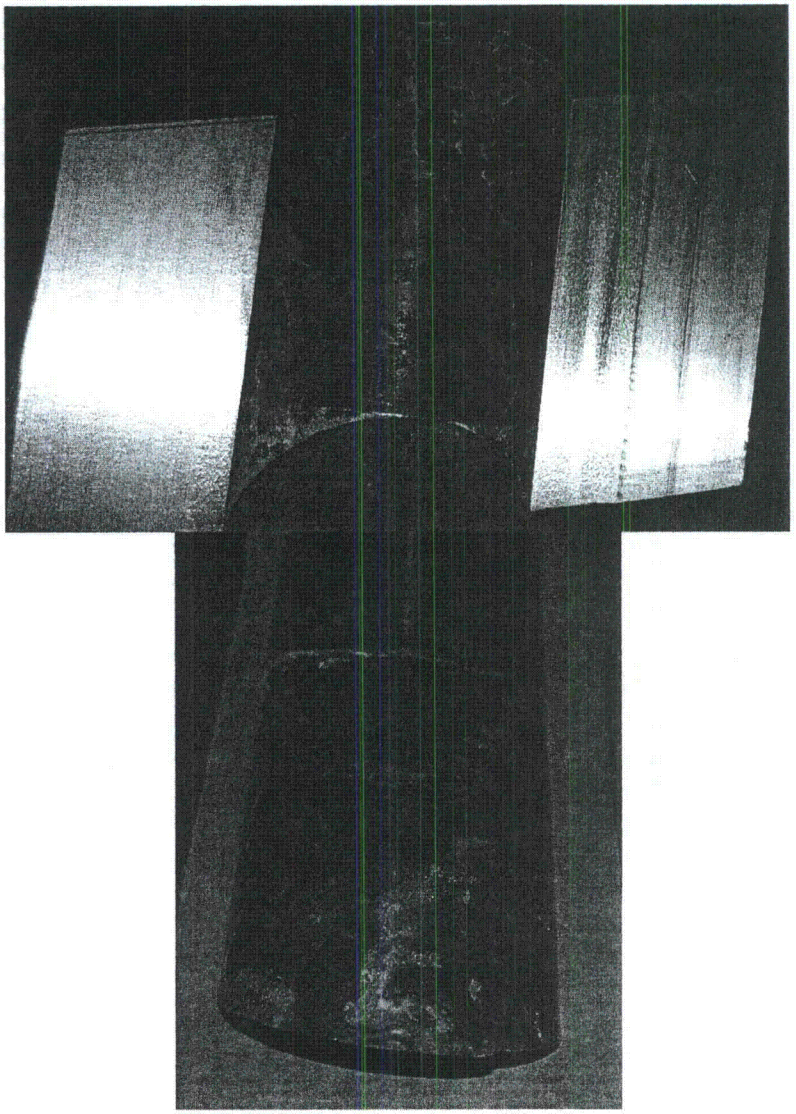

Figure 6.11 Exposed RPV Head and Nozzle from Low-Side Section

7 Correlation of Ultrasonic and Destructive Results

This section compares the phased-array ultrasonic results to the visual results obtained by cutting through the nozzle assembly to reveal the interference fit surfaces. The nozzle outer diameter surface was photographed in 45-degree increments with the individual photographs cropped and stitched together to form the montage image in Figure 7.1. Some evidence of thin boric acid deposits is visible in the white regions while a thin corrosion layer is seen in the rust-colored regions. The red line marks the interference fit region.

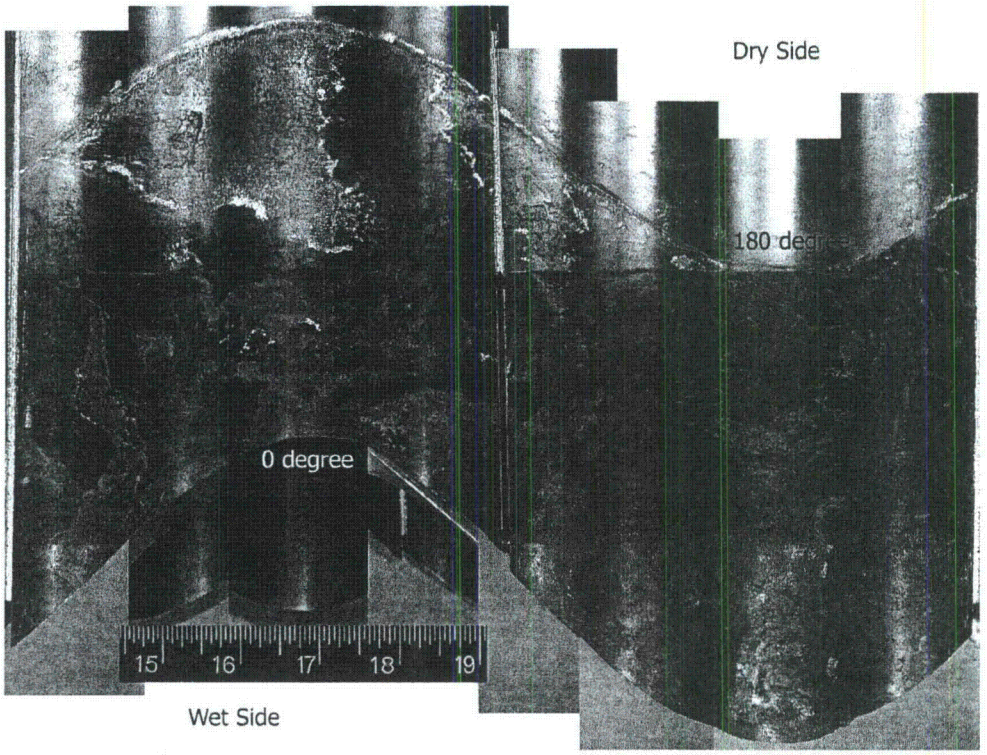

Figure 7.1 Nozzle Surface. The red line marks the interference fit region.

Similarly, the exposed reactor pressure vessel (RPV) head was photographed and the stitched image is displayed in Figure 7.2. The main leak path and other features seen in the ultrasonic images are clearly evident. Boric acid deposits are visible in white and corrosion products in the rust color. The interference fit region is evident in the photograph and is marked with the red line.

Comment [PGO54]: You may identify the leak path with an arrow or something on the figure.

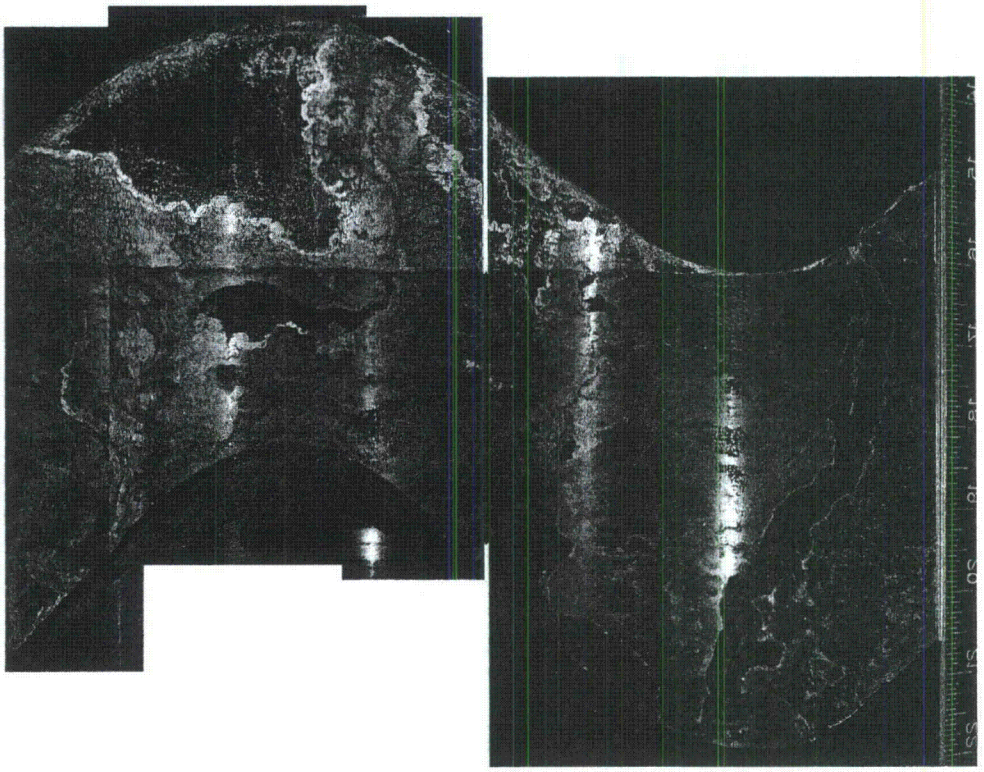

Figure 7.2 RPV Head Surface. The red line marks the interference fit region.

Comment [PGO55]: See comment on Figure 7.3 This picture should be on the same page as the UT data so that they can be easily compared.

A comparison of the ultrasonic and visual images is next presented. The ultrasonic data is overlaid on the RPV head montage photograph in a series where the opacity of the ultrasonic data is varied from 10 to 60%, in increments of 10%. Figure 7.3 displays the results with increasing opacity from left to right, top to bottom. The ultrasonic image was stretched to best fit the visual data but the match is not perfect due to the curved surfaces. Nevertheless, the ultrasonic features well match the features seen visually on the RPV head annulus. Clearly, the main leak path was precisely imaged and other partial leak paths are evident as well.

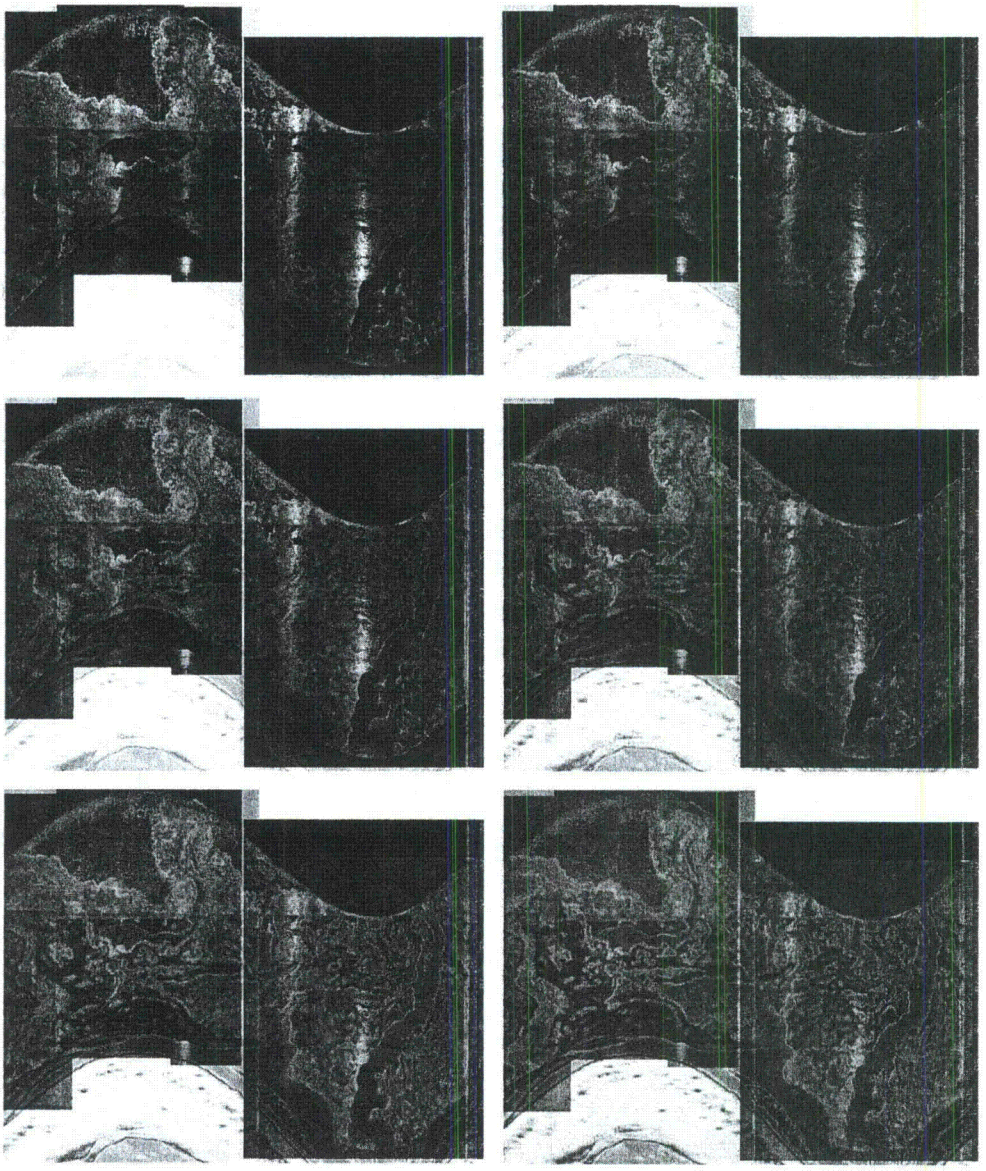

Figure 7.3 Ultrasonic Data Overlaid on RPV Head Photograph with Opacity Varying from 10 to 60%, Top to Bottom

Comment [PGO56]: You don't need all the overlaid images. We do need on the same page Figure 7.2 and the UT data on the same size scale next to each other, or one on top of the other.

8 J-groove Weld Examination

Comment [PGO57]: This section should be removed from the document.

As a supplemental evaluation, a J-groove weld examination was attempted using the same equipment as was used on the interference-fit evaluation. Ideally, a goniometer would have been included in the setup and thus allowed angled-beam inspections. Without a goniometer, the probe angle was fixed at zero degrees or normal to the inner diameter (ID) surface of the Alloy 600 tube. The zero-degree inspection of the weld was not ideal for detecting axial or circumferential cracks in a single elevation plane as any such crack presented only a knife edge view rather than a preferred side view. The evaluation was attempted on a best-effort basis.

Data were acquired in a single scan at probe focal depths of 20, 30, and 40 mm (0.79, 1.18, and 1.56 in.) to attempt to focus the beam into the weld material at different depths. All of the detected indications were located at the near surface of the weld, along the Alloy 600 tube-to-weld interface. As a result, these indications were better focused at the 20- and 30-mm (0.79- and 1.18-in.) depths as can be seen by comparing the circled indications in the three images in Figure 8.1. The top or 20-mm (0.79-in.) image has the largest amplitude response and resolves the two indications in the circled region. At the other extreme, the 40-mm (1.56-in.) focal depth image at the bottom shows a lower amplitude and blurred response from the same two indications.

A composite view of the ultrasonic indications in the weld are presented in the C-scan top view or plan view images in Figures 8.2 and 8.3 for the uphill and downhill halves of the weld, respectively. Each figure represents approximately 150 mm (5.91 in.) in the vertical or axial direction and 180 degrees in the horizontal or circumferential direction. The indications were generally all located at the Alloy 600 tube-to-weld interface, or near surface, as will be discussed in more detail below. These indications appear to be volumetric in shape, indicative of fabrication flaws and assumed to be welding anomalies. The types of fabrication flaws expected would include incomplete or lack of fusion between individual weld beads, inclusions, voids, etc. Notice that the downhill image contains more indications. This is not unexpected due to the more difficult configuration at this position in the nozzle assembly. One would be welding upside down, in a deeper cavity, and with limited access at this location; and therefore more likely to introduce imperfections in the weld. A connected string of indications following the curvature of the weld are observed in Figure 8.3—likely a lack of fusion between weld bead passes. These indications are noted by the red arrow in the figure.

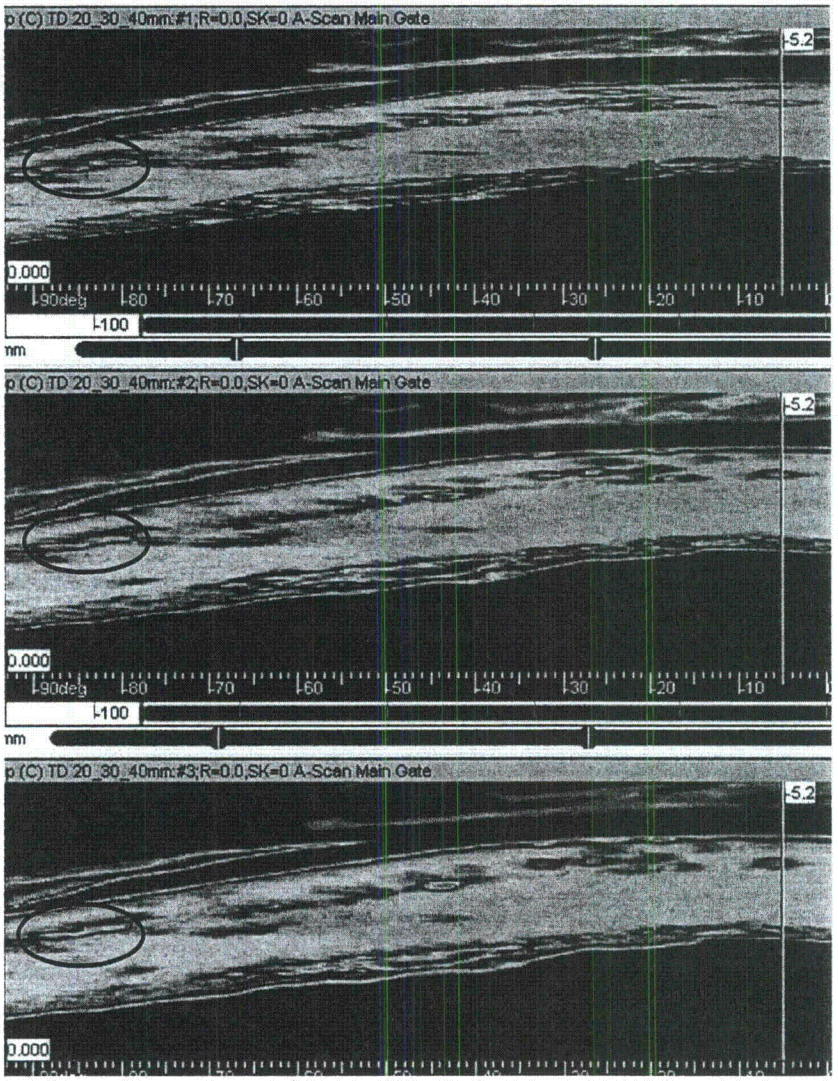

Figure 8.1 **Weld Images with Focal Depths at 20, 30, and 40 mm (0.79, 1.18, and 1.56 in.) from Top to Bottom, Respectively. The horizontal axis represents approximately 90 degrees and the vertical axis represents approximately 150 mm (5.9 in.). A 20-mm (0.79-in.) focus provided the best resolution in this data.**

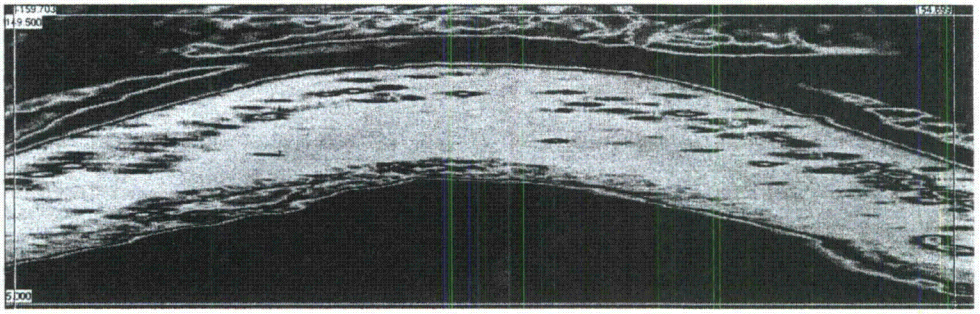

Figure 8.2 Uphill Half of the Weld. The horizontal axis represents approximately 180 degrees and the vertical axis represents approximately 150 mm (5.9 in.).

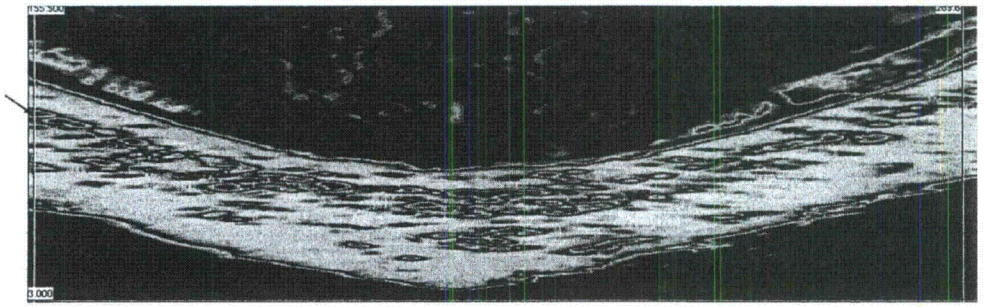

Figure 8.3 Downhill Half of the Weld. The horizontal axis represents approximately 180 degrees and the vertical axis represents approximately 150 mm (5.9 in.).

The ultrasonic indications were evaluated for flaw-depth position or distance into the weld material, and all responses appeared to be at or just below the surface with the surface representing the Alloy 600 tube-to-weld or butter interface. Figure 8.4 shows the composite top view of the downhill half of the weld with a vertical line drawn through the 174-degree position. A single plane or slice of data taken at the 174-degree position is displayed in Figure 8.5 and this figure represents a B-scan side view of the data. The horizontal axis in the side-view image represents depth or distance into the material. The first and second ultrasonic echoes are noted and represent reflections from the tube-to-weld interface. The scanner index or nozzle axis is shown in the vertical direction. The profile shape follows the front surface or inside of tube profile displayed in Figure 8.6. The distortion or deviation from vertical is due to the weld heating and subsequent cooling in the material and was measured at approximately 2 mm (0.08 in.). The distortion is magnified in the image due to the velocity difference between water and the Alloy 600 tube. Water velocity is nearly four times slower than the metal, assuming a water velocity of 1483 m/sec (58.4 in./msec) and 5820 m/sec (229.1 in./msec) for the metal. The side-view plots (Figures 8.5, 8.6, and 8.8) display the horizontal axis in units of distance

calculated with a metal velocity rather than in units of water velocity or time. During the data acquisition, a constant water path is assumed. As the water path varies due to the tube distortion, the difference is magnified by a factor of four on this metal scale. However, signals are correctly plotted relative to each other on the horizontal axis. For example, the first and second echoes are separated by a nominal distance of 17 mm (0.67 in.), which represents the tube wall thickness.

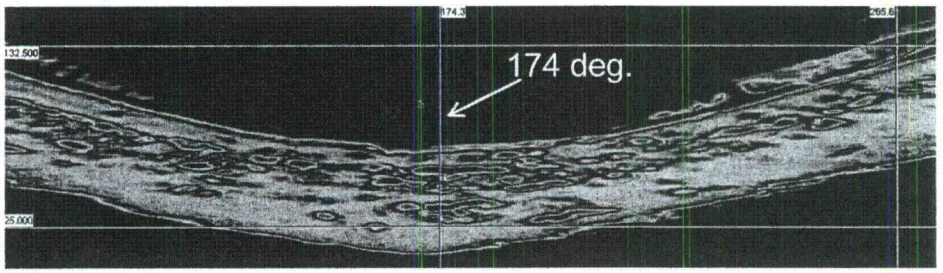

Figure 8.4 Location of Single Slice Shown in Figure 8.5. The horizontal axis represents 180 degrees approximately and the vertical axis 145 mm (5.7 in.).

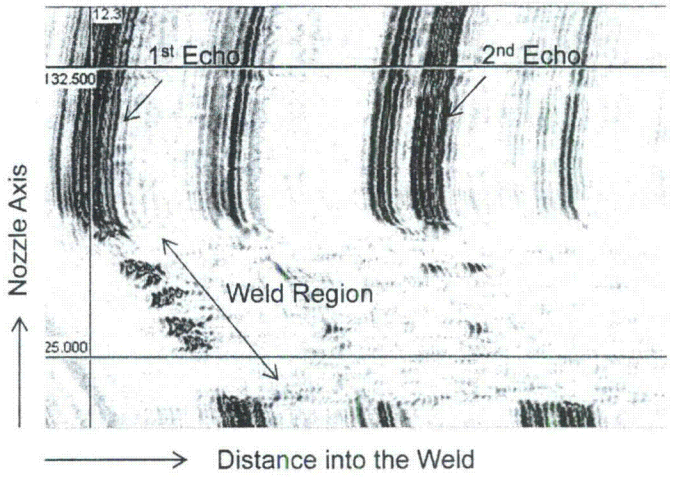

Figure 8.5 B-scan Side View at the 174-Degree Circumferential Position. Near-surface indications are visible in the weld material. The horizontal axis represents approximately 40 mm (1.6 in.) in metal and the vertical axis 155 mm (6.1 in.).

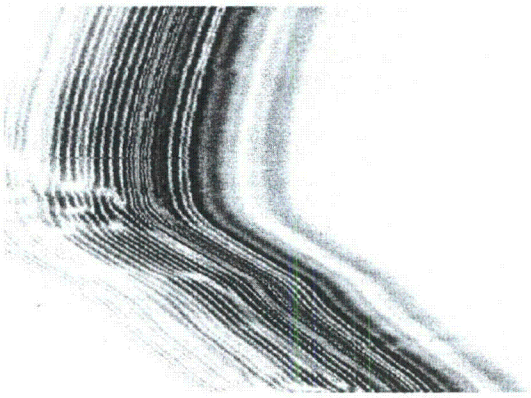

Figure 8.6 B-scan Side View of the Front Surface Echo Showing Surface Profile Distortion Due to Welding and Cooling at the 174-Degree Circumferential Position. The horizontal axis represents approximately 20 mm (0.8 in.) in metal and the vertical axis 155 mm (6.1 in.).

The weld region was evaluated for anomalies throughout the full 360-degree circumference. The indications fell along the Alloy 600 tube-to-weld interface at all but one circumferential position. At the 193-degrees position as noted in Figure 8.7, an indication appeared earlier in time than the other indications. The corresponding B-scan side view is shown in Figure 8.8 with the early indication circled. This earlier indication would plot into the tube material and could possibly be from a gouge in the tube and improper or no weld fill or repair. The indication displacement is shallow at approximately 1 mm (0.04 in.) in depth. No indications of circumferential cracking across or along weld beads were detected.

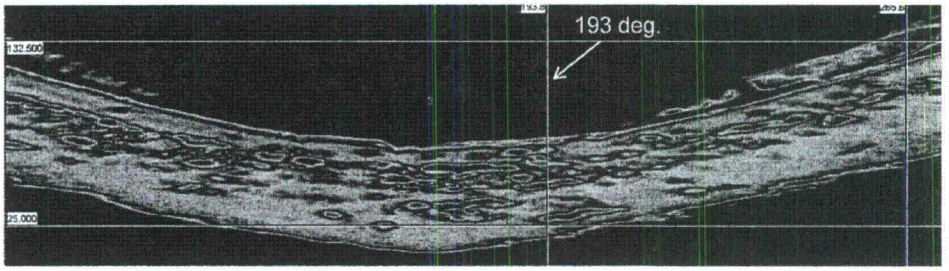

Figure 8.7 Location of Single Slice Shown in Figure 8.8

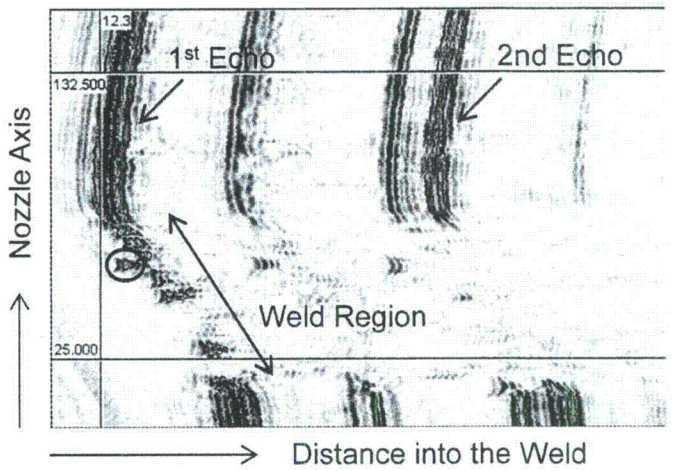

Figure 8.8 B-scan Side View at the 193-Degree Circumferential Position. Near-surface indications and one indication, circled in red, occurring earlier in time are visible. The horizontal axis represents approximately 40 mm (1.6 in.) in metal and the vertical axis 155 mm (6.1 in.).

A visual glimpse of several weld anomalies was made possible during the destructive evaluation conducted by Babcox &Wilcox. After making the dissection cut at approximately 95 and 275 degrees on the nozzle assembly, the exposed surfaces at 95 and 275 degrees were photographed with results shown in Figure 8.9 for the downhill half of the nozzle assembly. An enlarged version of the right side, or 95-degree position, is shown in Figure 8.10 and displays two flaws at the Alloy 600 nozzle-to-weld interface.

A comparison between the cut surface and ultrasonic data was made. It was observed that the 180-degree or low point on the weld was found to be located at 171 degrees in the ultrasonic image. Therefore, the ultrasonic data was shifted by 9 degrees to account for this offset. By this reasoning, the 95-degree cut surface corresponds to the 86-degree position in the ultrasonic data and the 275 cut surface corresponds to the 266-degree position ultrasonically. Again, note that these positions and the positions of the cut surfaces are estimated. The corresponding ultrasonic positions are noted in the ultrasonic C-scan top view image in Figure 8.11 with the left red vertical line at 87 degrees (on the left edge of the image) and the right blue vertical line at 266 degrees. The image did not extend to the 86-degree position so the 87-degree position is noted instead. The two indications marked by arrows at the 87-degree position in Figure 8.11 correlate to the two indications noted in Figure 8.10. An indication is also marked on the right side at the 266-degree position.

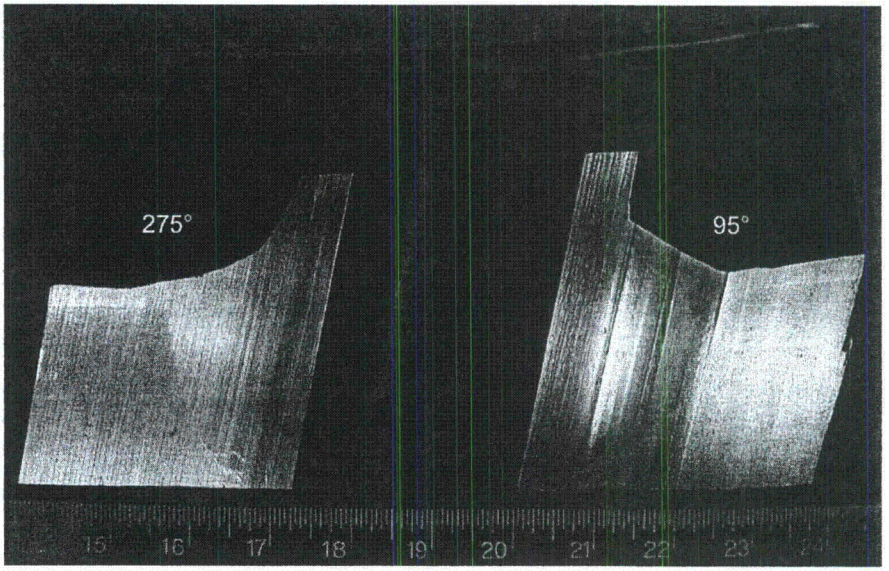

Figure 8.9 Cut Surfaces of the Nozzle Assembly at 95 Degrees on the Right and 275 Degrees on the Left. The scale is in inches.

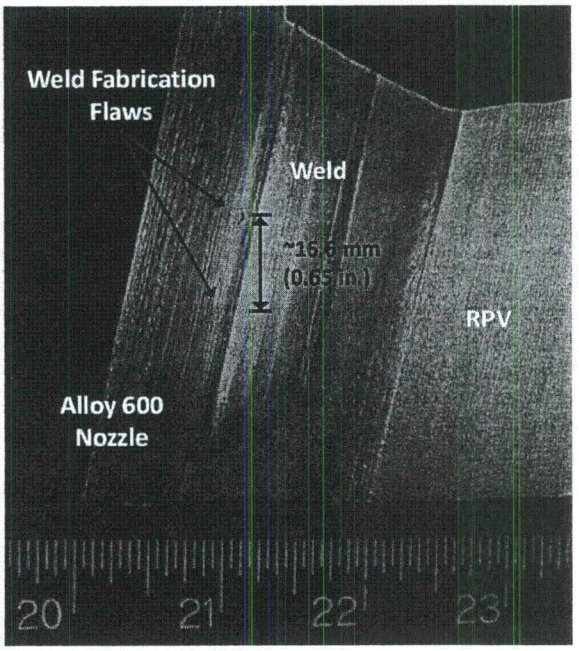

Figure 8.10 The 95-Degree Surface Shows Two Fabrication Flaws at the Alloy 600 Tube-to-Weld Interface

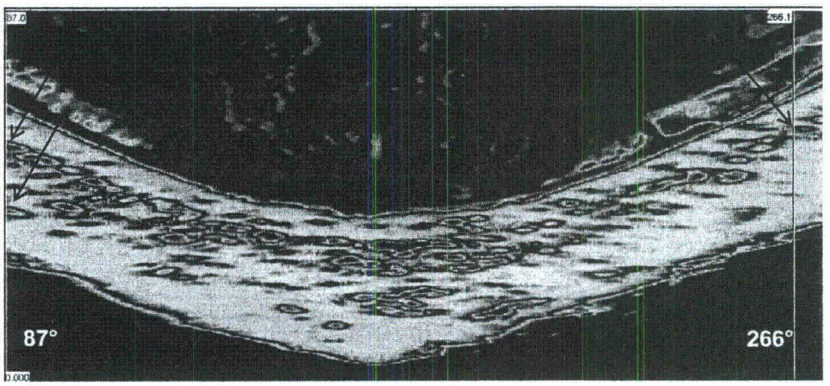

Figure 8.11 C-scan Top View of the Downhill Section of the Weld with the Left Edge Red Line and Right Side Blue Line Slicing through the Image at Locations Corresponding to the Cut Surfaces in Figure 8.9. The horizontal axis represents 180 degrees and the vertical axis 155 mm (6.1 in.) approximately.

B-scan side view images are displayed in Figure 8.12 for the 87- and 266-degree positions from Figure 8.11. The left side view image in Figure 8.12 at the 87-degree circumferential position shows the two defects with anomalous signals in between. The right image at the 266-degree position shows two possible defects with much lower signal amplitude, indicating smaller flaws.

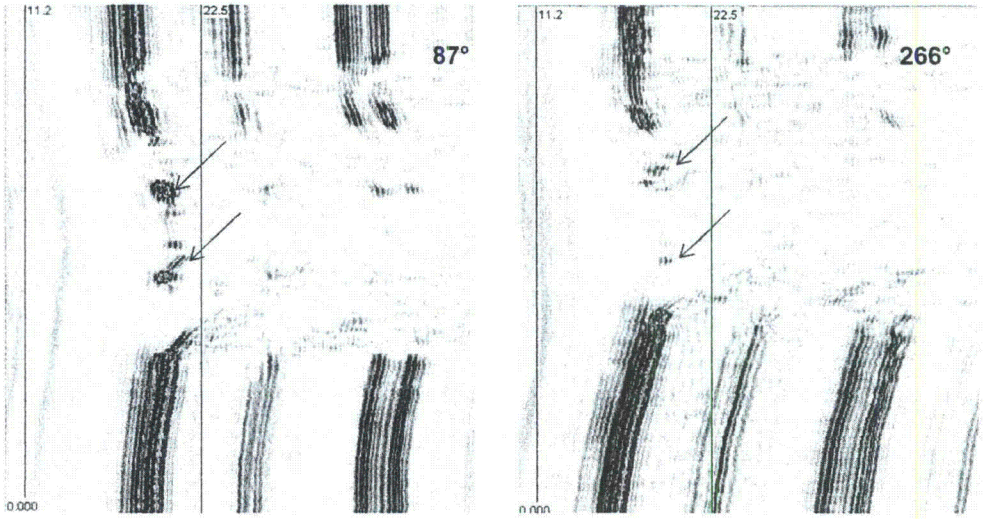

Figure 8.12 B-scan Views of the Data at 87 Degrees on the Left and 266 Degrees on the Right, Corresponding to the Cut and Exposed Surfaces in Figure 8.9. The horizontal axis in each image represents 40 mm (1.6 in.) in metal and the vertical axis represents 155 mm (6.1 in.) approximately. Flaw indications in the Alloy 600 tube-to-weld interface are noted with arrows.

The presence of these flaws was further confirmed by the dye penetrant test results on the cut surfaces shown in Figure 8.13. The two flaws at the 95-degree and two at the 275-degree cut surfaces are marked with arrows. Furthermore, two additional flaws in the weld material are circled on the 95-degree surface. These weld flaws were not evident in the ultrasonic data for two likely reasons. First, the beam possibly did not focus well at those depths. Second, any flaws occurring earlier in time (depth) would return or reflect the ultrasonic energy causing a shadow region beyond or later in time (depth) that would not be insonified.

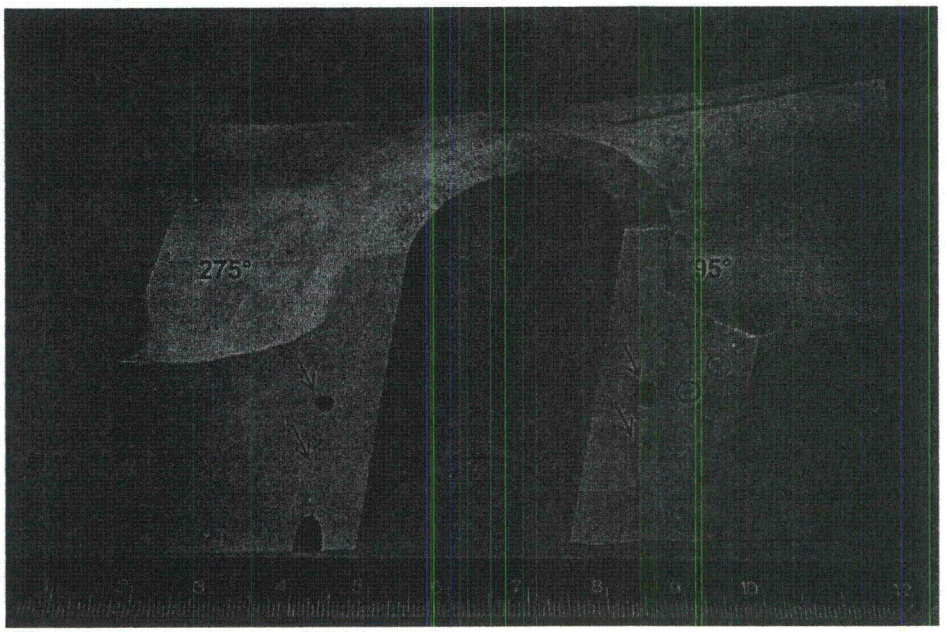

Figure 8.13 Dye Penetrant Test Results on the Downhill Dissection Cut Surface. The scale is in inches.

In summary, a J-groove weld examination was conducted with the probe oriented normal to the Alloy 600 tube inner surface. This was the same configuration used in the interference fit evaluation and was the only easily available option for a weld inspection. Inspections at several focal depths were made to attempt to fully insonify the weld material. The normal orientation was not ideal for detecting cracks as the beam was oriented toward an expected flaw edge rather than broadside to the flaw. The evaluation did not find any crack-like indications. Many fabrication flaws or weld anomalies were found with a higher concentration noted at the downhill side of the weld. The flaws mapped to the tube outer surface-to-weld interface region. Dye penetrant results validated four flaws at the tube-to-weld interface but also revealed two possible flaws in the weld that were not found ultrasonically. The larger of these two indications was in a shadow region caused by an earlier indication.

9 Additional Physical Measurements on the Reactor Pressure Vessel Head

As part of a supplemental study, attempts were made at measuring the boric acid thickness in the annulus as well as the extent of corrosion of the reactor pressure vessel (RPV) head. These measurements were then compared to the ultrasonic data. The boric acid thicknesses were first measured at specific points using an eddy current thickness gage. Next the RPV head surface was replicated with a Microset material, and boric acid thickness measurements were made on cross-sectional slices through the replica in the main leak path area. Finally, the replicated sections were examined with a stereomicroscope providing an indication of the corrosion extent. Best-effort attempts within limited budget and time constraints were made to remove the boric acid deposits in order to then measure corrosion or material wastage under the deposits. This effort was unsuccessful, but replica observations indicated minimal corrosion and wastage of the low-alloy steel head.

9.1 Boric Acid Measurements – Thickness Gage

In addition to the comparison of the interference fit region photographs with the ultrasonic images, a further study was conducted to obtain boric acid thickness measurements on the RPV head in the annulus region and to compare these results to the ultrasonic data. This was done while recognizing that the ultrasonic response in terms of reflected ultrasonic amplitude from the interference fit region would likely not correlate solely to the boric acid thickness measurements on the RPV low-alloy steel material. The boric acid on the RPV head material was only part of the contribution to the ultrasonic response. Also contributing to the ultrasonic response was the boric acid on the nozzle material (refer to Figure 7.1), and this contribution was not measured. Additional factors not measured or investigated were the density of the boric acid deposits and the low-alloy steel corrosion products which were visible in the photographs and could reflect or transmit ultrasonic energy differently than boric acid alone. Nevertheless, a best-effort attempt was undertaken to quantify the boric acid in the annulus region and relate these measurements to the ultrasonic data.

An eddy current probe was selected (DeFelsko PosiTector 6000 Series coating thickness gage) to measure the boric acid deposit thickness at selected points in the annulus region on the RPV head material. The probe had a point contact area of 1 mm (0.040 in.) in diameter and spanned a measureable coating thickness range of 0 to 45 mils (0 to 1.14 mm). The selected measurement sites were chosen to represent the differing ultrasonic amplitudes in the interference fit that included the main leak path, other partial leak paths, the interference fit with and without suspect boric acid present, and areas outside of the interference fit. A total of 70 points were selected by both Pacific Northwest National Laboratory (PNNL) and U.S. Nuclear Regulatory Commission (NRC) personnel and are displayed in Figure 9.1 for the photographed uphill and downhill halves of the RPV head. Figure 9.2 shows the ultrasonic data with a low opacity level superimposed on the photograph. A tri-color amplitude scale previously developed during the mockup study was used in the ultrasonic image and is displayed in the figure. Areas of interest were selected from the three color regions and represented a segmentation of ultrasonic responses. These specific points are associated with the green dots.

Comment [PGO58]: Is there a standard or some calibration informatoin that we can use to support the resolution of the probe.

The red dots were selected to represent the main leak path and other partial leak paths or bare metal regions. Lastly, the yellow dots were additional data points chosen for further clarification, such as the two pairs on either side of the uphill interference fit.

Comment [PGO59]: This needs to be restated because it is confusing as written. Particularly because the tricolor image used blue, light blue, and white to distinguish the regions. Should say something like, "Red dots represent measurement sites in and around the main and suspected leakage paths. Yellow dots represent measurement sites…,Green dots represent measurement sites…"

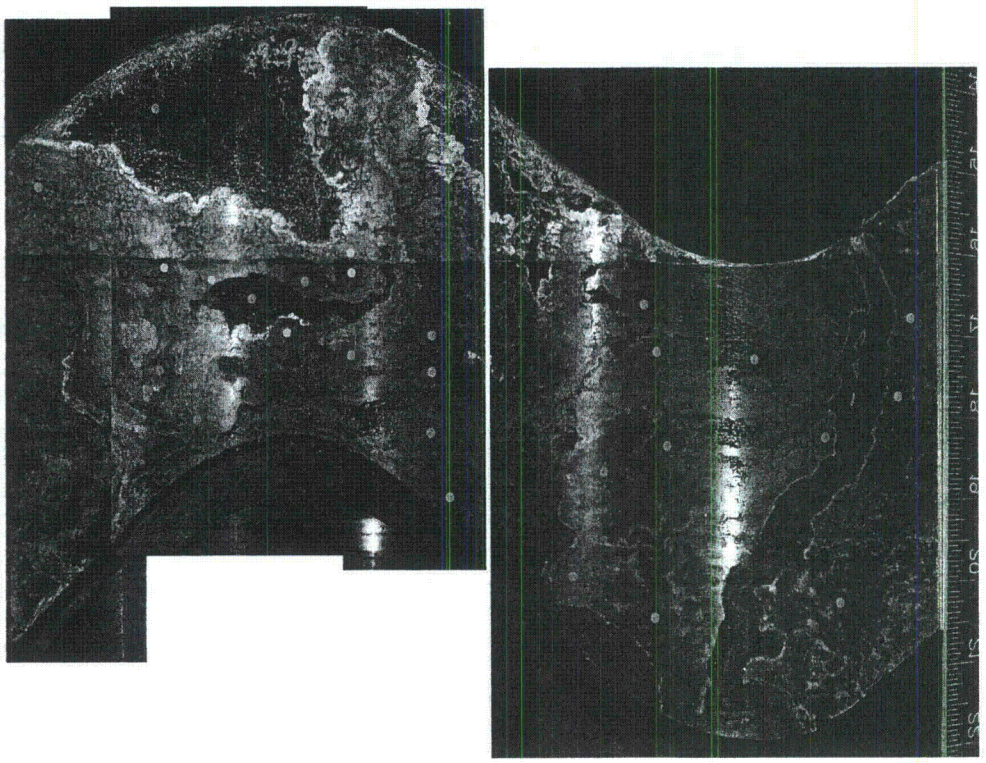

Figure 9.1 Photograph of the RPV Head Material with Boric Acid Measurement Points

Comment [PGO60]: State what the dots are and the significance of the color scheme. Mark the span of the interference fit.

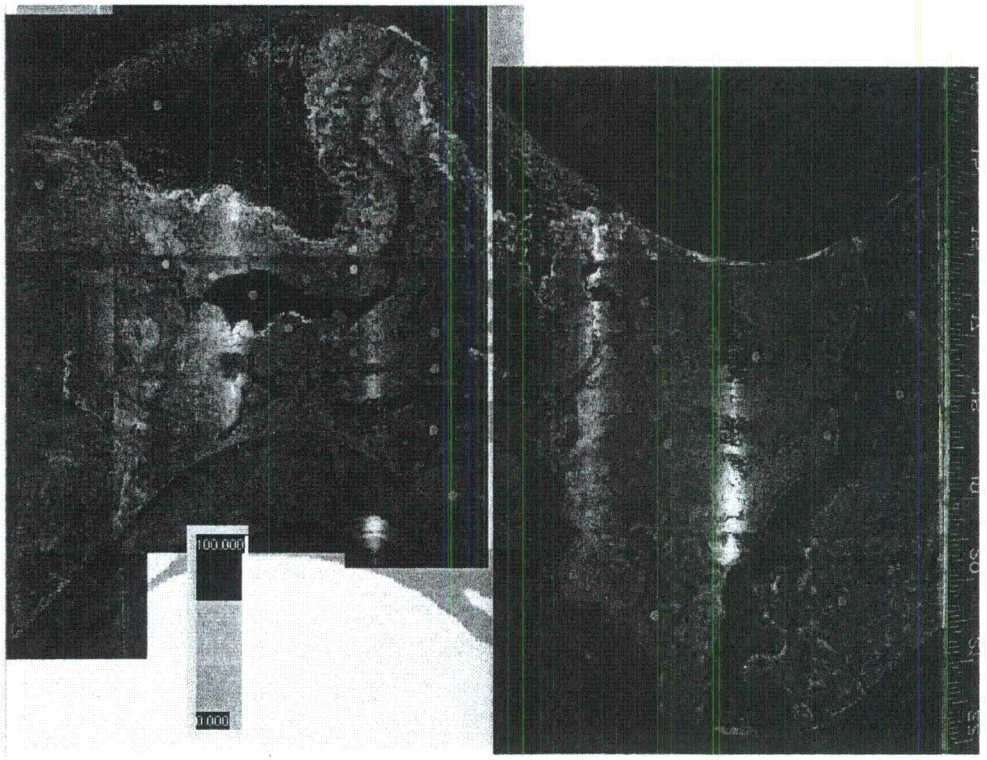

Figure 9.2 Ultrasonic Data with Boric Acid Measurement Points

Each of the 70 data points was numbered and the boric acid measurements were entered into a spreadsheet. The thickness measurements in microns are displayed adjacent to the data points in Figure 9.3. Some general observations were:

1) Boric acid values above and below the interference fit region outside of leak path and bare metal or nearly bare metal regions are nominally in the 130 to 200 micron (5.1 to 7.9 mils) range.

2) The two pairs of data (yellow dots) on either side of the interference fit on the uphill section show boric acid values of 156 and 150 microns (6.1 and 5.9 mils) above the fit region and 62 and 74.5 micron (2.4 and 2.9 mils) in the fit region.

3) Leak path and bare metal or nearly bare metal points have a thin surface corrosion layer, not visible boric acid deposits, with deposits at 16 microns (0.63 mils) or less.

Comment [PGO61]: Remove this figure

Comment [PGO62]: Section 9.1 needs to be rewritten from here forward. As presented, the data are confusling and are difficult to draw conclusions. The most important data to emphasize are the two horizontal line measurements across the leak path. Directly outside the leak path, the measurement sites show large thickness relative to the measurements inside the leak path. Even the "island" in the leak path shows the higher thickness. Going across these lines, there is a direct correlation between the amplitude response and the thickness measurement. We need to make a plot showing only those horizontal line data, where the amplitude is plotted vs. thickness. These data suggest that a leak path can be identified by a signal response of high amplitude with sharp decrease to low amplitude on either side. This is a useful observation for technicians and needs to be explicitly stated.

Point 2 to make, comparing the two horizontal measurement lines, as well as the other data points, the deposit thickness is lower inside the interference fit than in the counter bore. This is consistent with expectation that there is less gap in the annulus in the interference fit at operating temp. UT data generally show blue (low amplitude) response to the left and right of the leak path in the interference fit region and yellow/green (intermediate) to the left and right of the leak path below the interference fit. This may support the conclusion that there is a more compact deposit outside the leak path in the interference fit region that transmits energy better. You can almost tell the vertical span of the interference fit I the UT data by looking at the blue responses.

These are the results to emphasize. I will send some sample plots.

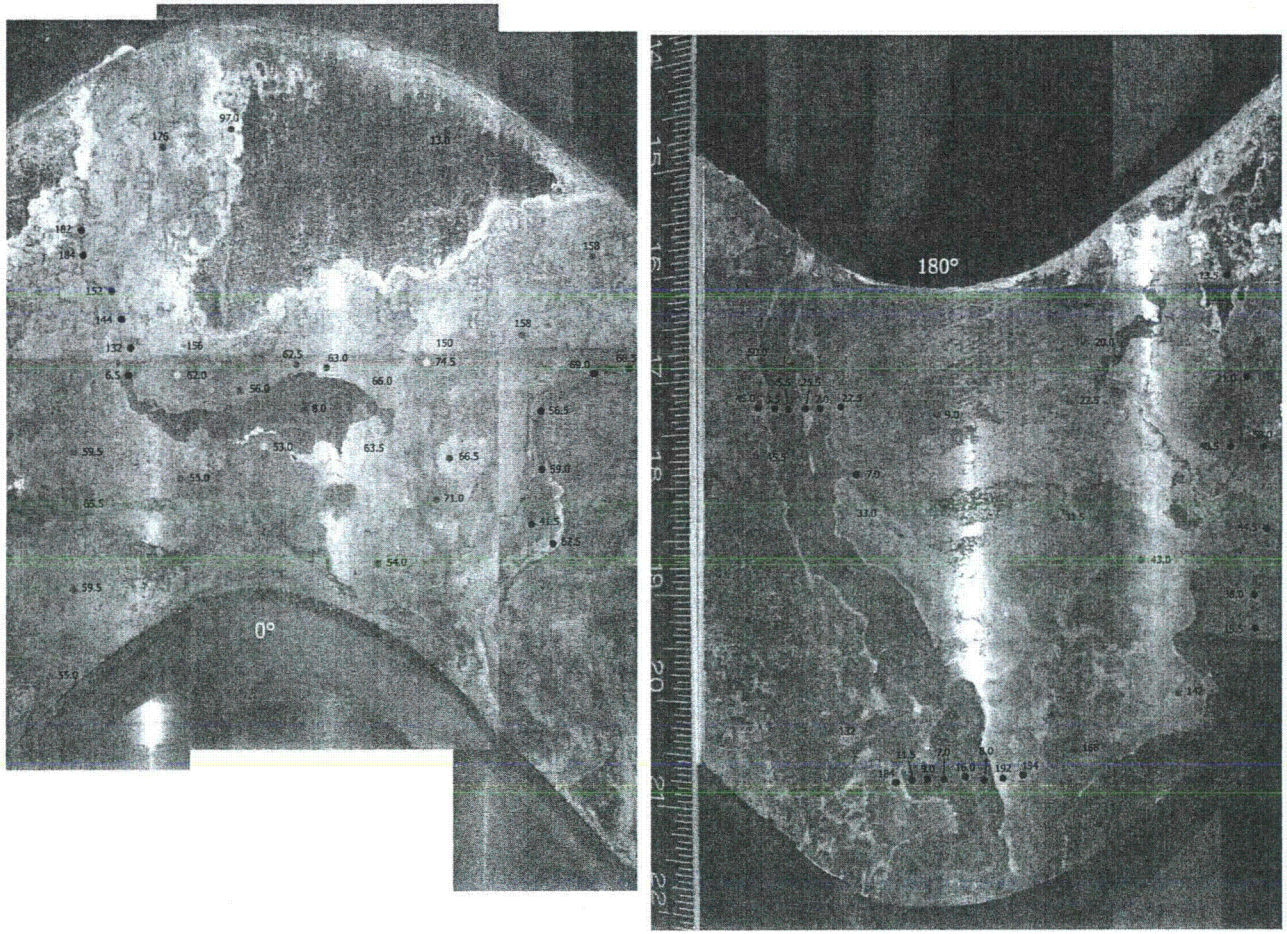

Figure 9.3 Boric Acid Thickness Values in Microns

Comment [PGO63]: The numbers are small and hard to read. Is there a way to make larger?

The relationship, if any, between the ultrasonic response values and boric acid values are displayed in graphical form in Figures 9.4 and 9.5. In the first graph, shown in Figure 9.4, the ultrasonic data are displayed as a function of the boric acid values for measurement points in the interference fit region. The points circled in the upper left corner represent bare metal or nearly bare metal points and point from the leak path. These points cluster separately from the remaining data and have ultrasonic values greater than 65% of full screen height and coating layer values less than or equal to 9 microns (0.35 mils). Furthermore, these points represent a strong ultrasonic response such as one associated with a reflection from a gap or void in the interference fit region. There was not close contact between the Alloy 600 tube outer diameter (OD) and the RPV head inner diameter (ID) materials at these locations and minimal or no boric acid or corrosion products were present. The points outside of the circled region represent the rest of the data and show no correlation between the ultrasonic response and the boric acid or coating thickness. The region is, however, bounded by boric acid deposits in the 16 to 75 micron (0.63 to 3.0 mils) range, while the ultrasonic responses almost cover the full range, spanning from 10 to 80% of full screen height.

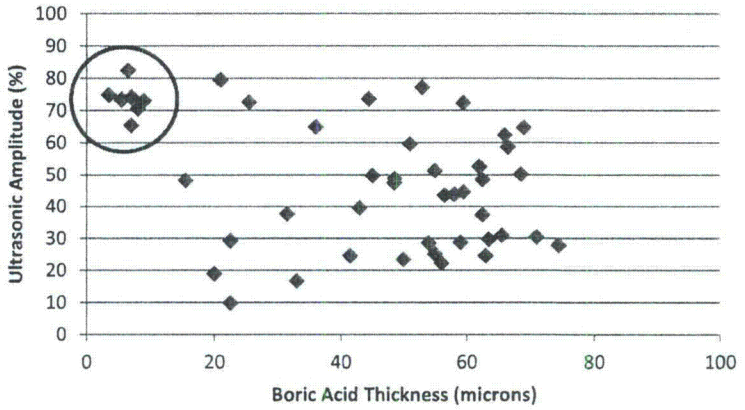

Figure 9.4 Ultrasonic Amplitude as a Function of Boric Acid Thickness from Points in the Interference Fit Region

Comment [PGO64]: Remove figure.

The data above and below the interference fit are displayed in Figure 9.5. The leak path or bare metal points are circled and have ultrasonic values between 69 and 87% and boric acid or corrosion thickness values of 16 microns (0.63 mils) or less. Outside of this circled cluster and the one isolated data point in the middle, the remaining data have boric acid thickness between 132 and 192 microns (5.2 and 7.6 mils) and ultrasonic amplitudes between 48 and 83%. The one outlier point is from the dry side on the uphill half and is towards the edge of a boric acid patch with a center-of-patch (0.7 in. or 17.8 mm to the center) thickness of 176 microns (6.9 mils).

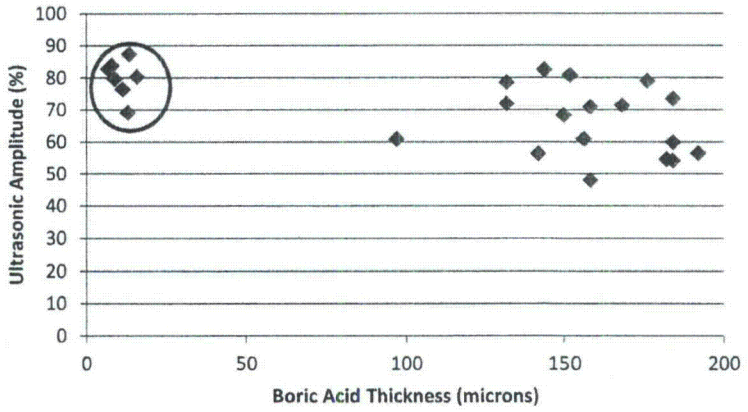

Figure 9.5 Ultrasonic Amplitude as a Function of Boric Acid Thickness from Points Above and Below the Interference Fit Region

Comment [PGO65]: Remove figure.

If this outlier or transitional point from Figure 9.5 is excluded, all of the boric acid measurements can be segmented into three categories. The leak path or bare metal regions have approximately less than 16 microns (0.63 mils) of boric acid/corrosion products. The interference fit points contain between 16 and 75 microns (0.63 to 3.0 mils) of boric acid, and the annulus region above and below the interference fit contain 132 to 192 microns (5.2 to 7.6 mils) of boric acid. These numbers are assumed to depend on the geometry of the particular control rod drive mechanism (CRDM) assembly and more specifically on the size of the interference fit and counter bore regions outside of the interference fit. It is reasonable to assume that with a leak, any interference fit or counter bore gap could fill with boric acid and corrosion products.

Attempts to correlate the ultrasonic data to the RPV head boric acid data are again simplistic. The ultrasonic responses were sensitive to the entire interaction at the Alloy 600 tube-to-steel RPV head interface including metal-to-metal contact or lack of contact, boric acid and corrosion product presence, and the density of these materials. The earlier proposed tri-level segmentation of ultrasonic responses based on the mockup specimen was inadequate. It was proposed from the ideally machined mockup with well-mated surfaces. In an actual nozzle, the contact area could be as low as 5% at operating temperatures due to out-of-roundness, not straight components, and surface roughness (Hunt and Fleming 2002). Furthermore, the mockup did not contain a counter bore region. Less-than-perfect data registration also likely contributed to error in the correlation between the ultrasonic and boric acid values. The ultrasonic images show large variations between points located in close proximity to each other. Small positional errors in the boric acid measurement could have led to an incorrect matching of the data. An overlay of the ultrasonic data on the RPV head with the 70 measurement points is shown in Figure 9.6 with the multilevel color scheme for reference. The ultrasonic responses in the leak path and bare metal regions are greater than 65%, while interference fit data are in the 10 to 80% range and counter bore data are in the 48 to 83% range. High values, large

reflectance, indicate an interface with a large impedance mismatch such as metal to air. Low values indicate good transmission at the interface due to similar materials tightly bonded. Bare metal and leak path points show large ultrasonic reflectance with a minimal corrosion layer. These data points cluster well. The interference fit data does not. Approximately two-thirds of the interference fit ultrasonic data are below the 50% response level and cluster with boric acid values in the 16 to 75 micron range (0.63 to 3.0 mils). The remaining one-third of the ultrasonic data has response levels in common with the counter bore data. Because a full investigation of the multiple factors affecting the ultrasonic responses was beyond the scope of this project, the data are at best bounded but do not show a direct correlation to the boric acid measurements on the RPV head.

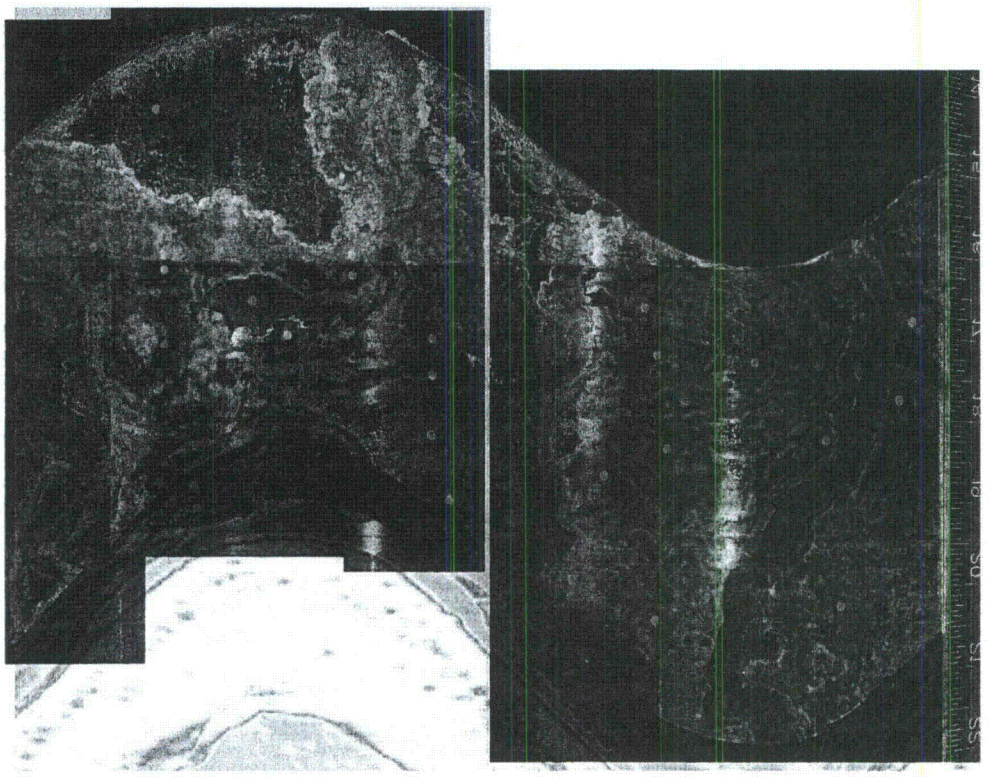

Figure 9.6 Overlay of Ultrasonic Image on the 70 Measurements Points

Comment [PGO66]: Remove figure.

9.2 Boric Acid Measurements – Microset Cross Sections

Confirmatory boric acid measurements were also visually made on Microset replicas of the RPV annulus in the main leak path region. This replicating material has better than 0.1 micron (0.004 mils) resolution. Eight areas of interest across the main leak path, as shown in Figure 9.7, were selected for these additional and confirmatory measurements. The sliced and annotated replica is shown in Figure 9.8. Boric acid measurements were made on the edges of the slices with the white arrows showing the cut surfaces that were measured. Several of the measurement values obtained by these surface cross sections were compared to the thickness gage measurements. While only a few data points were compared and these occurred at thicknesses of approximately 40 and 175 microns, the data showed good agreement as Figure 9.9 shows. Ideally, comparisons in the middle of this range, nominally 120 microns, would have been made as well. However, for this best-effort work, several measurements were validated.

Comment [PGO67]: State that these include the horizontal line measurement locations through the leak path discussed in the previous section.

Comment [PGO68]: Do you have any of the profile pictures?

Comment [PGO69]: Restate this to say that the comparisons were done for the measurements across the leak path.

Comment [PGO70]: Do not say this.

9.3 Replicated Surfaces – Stereomicroscope

Comment [PGO71]: Only emphasis for this section is that machining marks were evident in the leak path. That suggests low flow rate/minimal wastage. The

Lastly the replicated surfaces from Figure 9.8 were viewed with a stereomicroscope to better document the surface conditions and to attempt to quantify the corrosion or erosion of the low-alloy steel in the annulus region. Machining marks were observed on the replicated surfaces indicating minimal corrosion, erosion, or wastage throughout the leak path region. Interesting areas are discussed.

Figure 9.10 shows replica pieces 2 and 3 in the main leak path in the region below the interference fit. Both pieces show double streaks from corrosion product staining but no or minimal actual corrosion or wastage. The machining marks are intact across the images.

The transition from below the interference fit to the interference fit region is captured in Figure 9.11 on piece 4. Machining marks are clearly evident and were observed in most of the bare areas examined on the RPV head surface. The surface finish within the interference fit region was approximately equivalent to a turned finish of 63 microinches. The finish below the interference fit region was approximately equivalent to a milled 63 finish.

Comment [PGO72]: What does this mean?

Piece 5 contained an angular feature or anomaly with an approximate length of 2.3 mm (0.090 in.) and is shown in Figure 9.12. The right image is at a twice the magnification as the image on the left and shows more detail. This feature appeared to be more of a dent or scrape and not corrosion. Piece 5 lies in the interference fit region.

The only corrosion observed in the replicated surfaces was in the region above the interference fit in piece 9. The piece is shown in Figure 9.13 with the two areas of interest circled. The circled region on the left was in the main leak path and covered an area of approximately 6.4 mm (0.25 in.) in diameter with a depth of 0.25 mm (0.01 in.). The corroded area on the right was approximately 12.7 by 1.6 mm (0.5 by 0.06 in.) with a depth of 0.25 mm (0.01 in.).

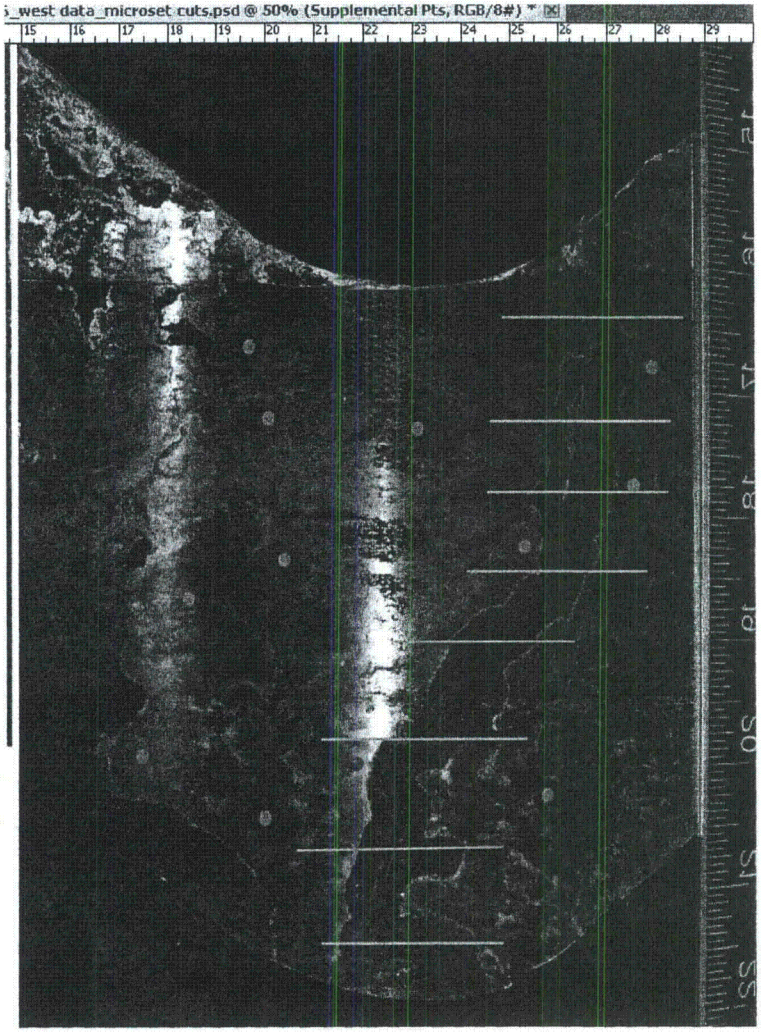

Figure 9.7 **Eight Areas Selected for Boric Acid Thickness Measurements on Cross-Sectional Slices of Microset Replica**

Comment [PGO73]: Remove dots from figure except those for the horizontal line measurements.

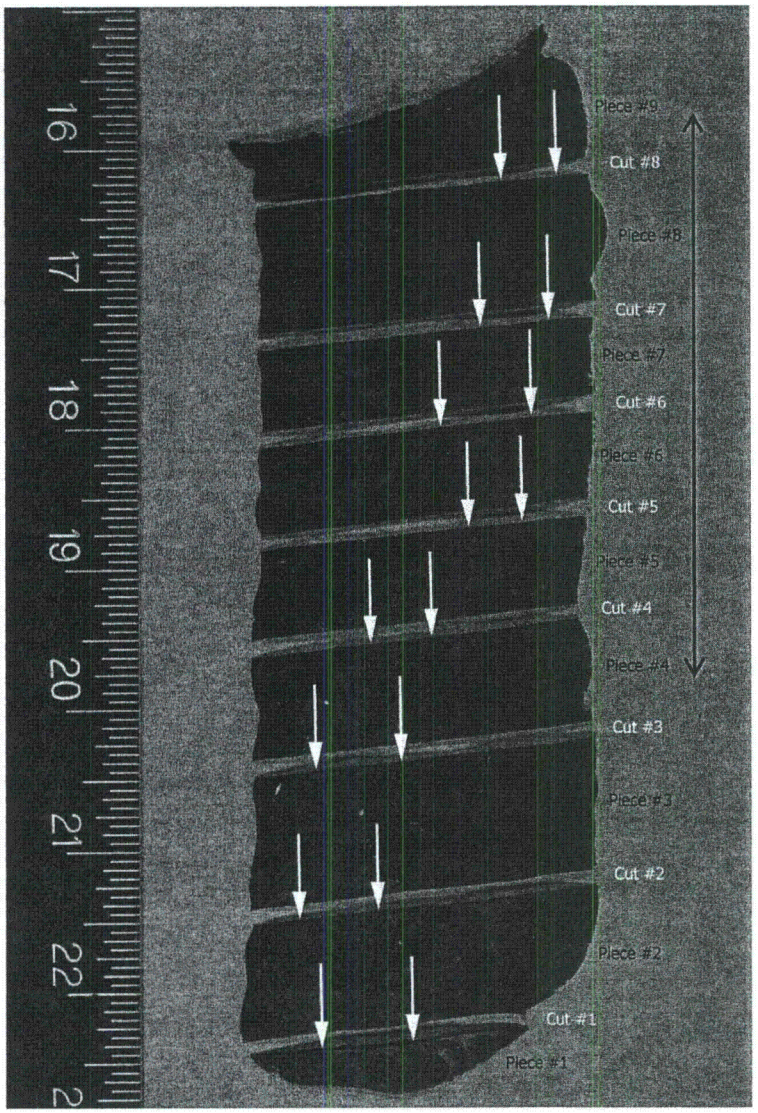

Figure 9.8 Leak Path Replica with Cuts and Pieces Identified. The interference fit region is noted with the black line and is contained in pieces 4 through 9.

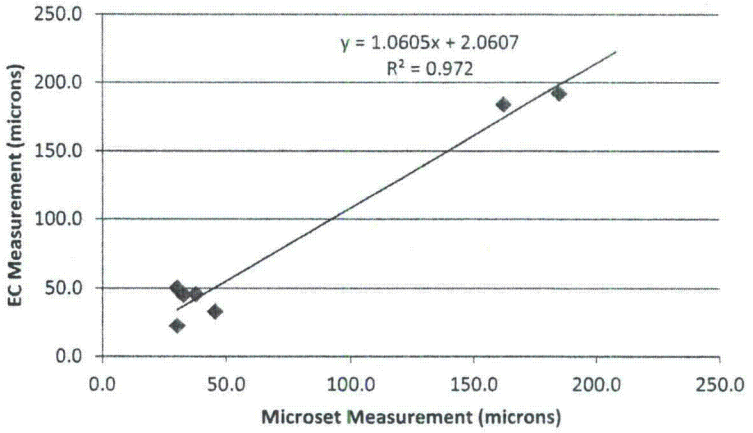

Figure 9.9 Eddy Current Thickness Gage and Microset Thickness Measurements of Boric Acid Comparison

Comment [PGO74]: Use a table to compare the measurements instead of plot.

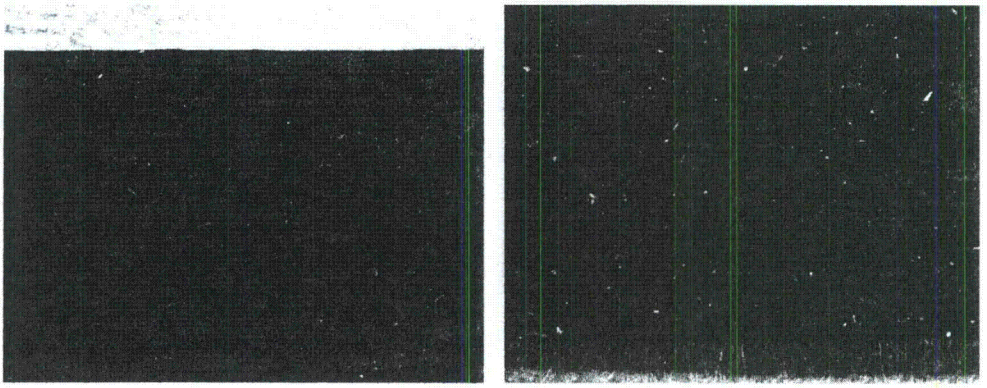

Figure 9.10 Staining Streaks in the Leak Path Below the Interference Fit from Replica Pieces 2 and 3, Left and Right, Respectively. The red line represents 2.0 mm (0.80 in.) in length.

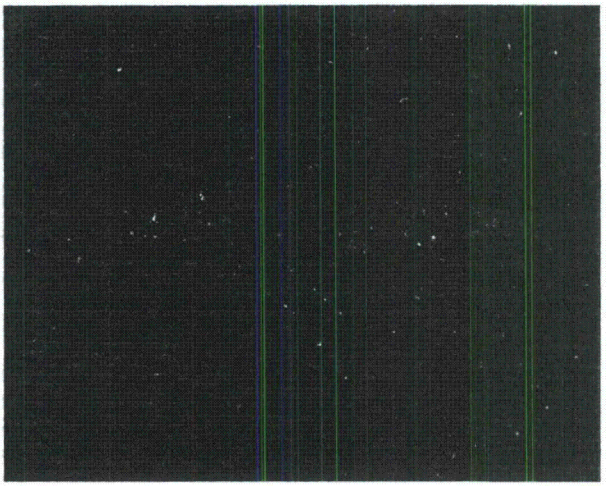

Figure 9.11 Transition from Below the Interference Fit to the Interference Fit Region. Machining marks are evident in this replica piece 4. The red line represents 2.0 mm (0.80 in.) in length.

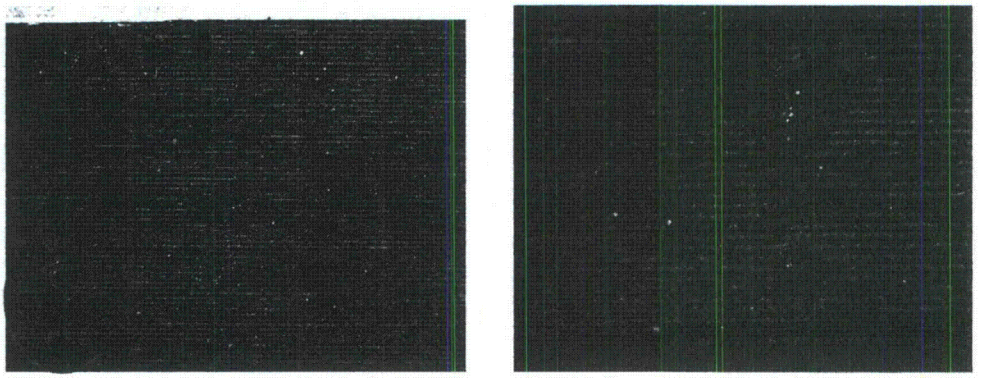

Figure 9.12 Piece 5 from the Interference Fit Region Shows an Indication of a Scrape. In the left image the red line represents 2.0 mm (0.80 in.) in length. The image on the right at twice the magnification of the left shows more detail.

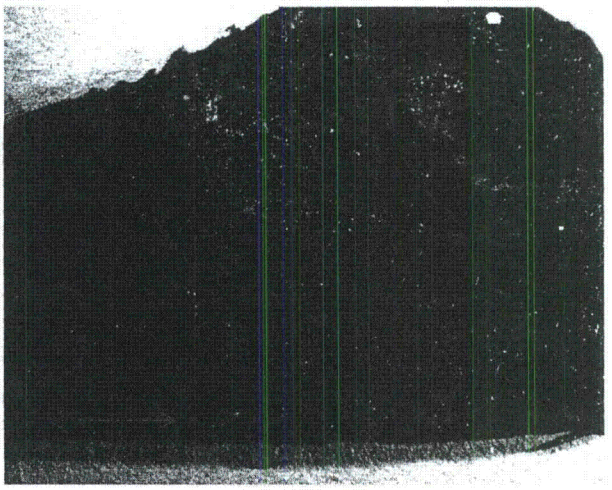

Figure 9.13 Corrosion Areas Observed Above the Interference Fit Region. The red line represents 2.0 mm (0.80 in.) in length.

In summary, a limited boric acid thickness measurement study was conducted on the RPV head material. Boric acid deposits were found throughout the interference fit region as well as above and below this region. Larger boric acid thickness values were found in the counter bore regions above and below the interference fit and ranged from approximately 132 to 192 microns (5.2 to 7.6 mils). In the interference fit region itself, the boric acid values were in the 16 to 75 micron (0.63 to 3.0 mils) range. The leak paths and bare metal regions had a measureable corrosion layer of 16 microns or less. Finally, the ultrasonic measurements were sensitive to the entire interaction at the tube-to-RPV head interface so a simplistic comparison of boric acid thickness on the RPV head to ultrasonic response showed only a partial correlation.

10 Summary and Conclusions

In summary, a successful ultrasonic examination of the interference fit region of control rod drive mechanism Nozzle 63 from the North Anna Unit 2 power plant was conducted. A phased-array ultrasonic system was calibrated on a mockup specimen containing two interference fit regions. The probe spot size at the interference fit was modeled at 1.2 by 1.2 mm (0.04 by 0.04 in.) at the −6 dB level. Ultrasonic data from notches in the carbon steel material from one of the mockup interference fit regions showed system resolution at nominally 4 mm (0.16 in.) in both the axial and circumferential directions. Notches as shallow as 0.028 mm (0.0011 in.) were detected as well as notches as narrow as 0.80 mm (0.10 in.) in the circumferential direction. The second mockup interference fit contained regions with boric acid deposits. These regions were ultrasonically imaged and suggested that the ultrasonic responses could be segmented into three categories: 1) good interference fit, 2) interference fit with boric acid, and 3) leak path or gap.

Ultrasonic data were acquired on Nozzle 63 and clearly showed a variation of responses throughout the annulus region. The primary leak path at the downhill position of the nozzle was imaged and definitively spanned the annulus region thus providing a path for borated water to reach the top of the head. Partial leak paths were also identified. The normal beam inspection, while not optimum for crack detection, also detected two axial cracks in the nozzle. These cracks were previously found by industry with an eddy current examination conducted during an in-service inspection. One of the cracks was below the weld at the uphill position. The other axial crack was located above the weld at the downhill position, which also places it in the main leak path. A comparison of the Pacific Northwest National Laboratory (PNNL) ultrasonic data to that obtained by industry showed similar results but the PNNL data had better resolution, data registration, and focusing. Finally, a supplemental evaluation of the weld, which was again not optimized for crack detection, failed to detect any weld cracking but did detect numerous near-surface fabrication flaws.

After sectioning of the nozzle assembly to reveal the interference fit and photographing the exposed surfaces, the primary leak path was confirmed. Also confirmed was the excellent agreement of the ultrasonic images and exposed features on the annulus surfaces.

Additional measurements were made to quantify the thickness of the boric acid deposits or corrosion layer on the reactor pressure vessel (RPV) head. It was reasonable to assume that any gap in the annulus could fill with boric acid deposits. As the gap between Alloy 600 tube and low-alloy steel head varied so too did the boric acid thickness. The leak path or bare metal corrosion layer throughout the annulus was 16 microns (0.63 mils) or less with ultrasonic responses greater than 65%. Boric acid apparently did not deposit in the leak path due to the constant flow of borated water through the area, and the ultrasonic response indicates an air gap was present. The boric acid deposits in the counter bore regions above and below the interference fit were in the 132 to 192 micron (5.2 to 7.6 mils) range with ultrasonic responses between 48 and 83%. These two regions, leak path and counter bore, are clearly distinct from each other in both boric acid thickness but overlap in ultrasonic response. The interference fit region with a narrower annulus had boric acid deposits in the 16 to 75 micron (0.63 to 3.0 mils) range, in between the leak path and counter bore values. There was not a direct correlation

Comment [PGO75]: This needs to be revised and presented as a bulleted list, roughly as follows...

1. Nozzle 63 showed evidence of leaking in service and was removed from the North Anna head for analysis and testing.
2. Prior to testing the nozzle, mockup showed UT system capable of identifying corrosion/wastage and boric acid deposits in annulus region between nozzle and head. Wastage is distinguished by high amplitude UT response. Boric acid is distinguished by low amplitude UT response.
3. UT of the nozzle showed primary leakage path on downhill side, as identified by high amplitude response, and scattered boric acid deposits in annulus region, as identified by low amplitude response.
4. Destructive examination of the nozzle visually confirmed the presence of the leakage path and boric acid deposits identified in the UT.
5. Measurements of surface deposit thickness traversing the leak path showed a rapid transition from high thickness just outside the leak path, to low thickness in the leak path, and back to high thickness on the other side of the leak path. This corresponds to a rapid change in the UT response from low amplitude, to high, and low again. This suggests that this UT response would be characteristic of a well-defined leakage path.
6. Generally, the region of the interference gives a lower amplitude UT response compared to regions outside the interference fit. Surface deposit thickness measurements show thinner deposits in the interference fit, suggesting they are more compact and are more efficient for ultrasonic energy transfer.
7. Surface replication shows that machining marks are still visible in the leakage path, suggesting a low leakage rate that led to minimal wastage of the RPV head.

Please modify as you see necessary.

between the RPV head boric acid measurements in the interference fit region and the ultrasonic responses. This is not unexpected as the ultrasound was influenced by additional physical conditions that were not measured such as the deposits on the outside of the Alloy 600 tube surface and the density of any of the deposits.

Lastly, the leak path region of the RPV head was replicated and limited confirmatory measurements made on the replica for boric acid thickness. The replica surfaces were imaged with a stereomicroscope and showed minor evidence of corrosion product streaking and little or no corrosion or wastage. Machining marks were clearly evident across the main leak path. Two small areas with minor corrosion were found above the main leak path with depths of 0.25 mm (0.01 in.). Attempts to remove the boric acid deposits on the RPV head to determine wastage underneath were unsuccessful, but dental pick probing indicated that all areas were sound. Therefore, in this leaking nozzle assembly, there was minimal corrosion or wastage occurring on the low-alloy steel RPV head.

11 References

Bennetch JI, GE Modzelewski, LL Spain and GV Rao. 2002. "Root Cause Evaluation and Repair of Alloy 82/182 J-Groove Weld Cracking of Reactor Vessel Head Penetrations at North Anna Unit 2." In *2002 Proceedings of the ASME Pressure Vessels and Piping Conference (PVP2002), Service Experience and Failure Assessment Applications*, pp. 179-185. August 5-9, 2002, Vancouver, British Columbia, Canada. American Society of Mechanical Engineers, New York.

Clark AF. 1968. "Low Temperature Thermal Expansion of Some Metallic Alloys." *Cryogenics* 8(5):282-289.

Cumblidge SE, SR Doctor, GJ Schuster, RV Harris Jr., SL Crawford, RJ Seffens, MB Toloczko and SM Bruemmer. 2009. *Nondestructive and Destructive Examination Studies on Removed-from-Service Control Rod Drive Mechanism Penetrations.* NUREG/CR-6996, PNNL-18372, U.S. Nuclear Regulatory Commission, Washington, D.C.

Economou J, A Assice, F Cattant, J Salin and M Stindel. 1994. "NDE and Metallurgical Examination of Vessel Head Penetrations." In *3rd International Symposium on Contribution of Materials Investigation to the Resolution of Problems Encountered in Pressurized Water Reactors.* September 12-16, 1994, Fontevraud, France. French Nuclear Energy Society.

EPRI. 2005. *Materials Reliability Program: Destructive Examination of the North Anna 2 Reactor Pressure Vessel Head (MRP-142): Phase 1: Penetration Selection, Removal, Decontamination, Replication, and Nondestructive Examination.* EPRI Report 1007840, Electric Power Research Institute, Palo Alto, California.

EPRI. 2006. *Materials Reliability Program: Destructive Examination of the North Anna 2 Reactor Pressure Vessel Head (MRP-198): Phase 3: A Comparison of Nondestructive and Destructive Examination Findings for CRDM Penetration #54.* EPRI Report 1013414, Electric Power Research Institute, Palo Alto, California.

Gorman J, S Hunt, P Riccardella and GA White. 2009. "Chapter 44, PWR Reactor Vessel Alloy 600 Issues." In *Companion Guide to the ASME Boiler and Pressure Vessel Code, Volume 3, Third Edition*, ed: KR Rao. ASME Press, New York.

Grimmel B. 2005. *U.S. Plant Experience with Alloy 600 Cracking and Boric Acid Corrosion of Light-Water Reactor Pressure Vessel Materials.* NUREG-1823, U.S. Nuclear Regulatory Commission, Washington, D.C.

Hunt S and M Fleming. 2002. *Probability of Detecting Leaks in RPV Upper Head Nozzles by Visual Inspections, Revision 1, June 17, 2002.* Dominion Engineering, Inc., Reston, Virginia. Prepared for MRP PWR Alloy 600 Assessment Committee. U.S. Nuclear Regulatory Commission ADAMS Accession No. ML030860192.

IAEA. 2007. *Assessment and Management of Ageing of Major Nuclear Power Plant Components Important to Safety: PWR Pressure Vessel Internals, 2007 Update.* IAEA-TECDOC-1556, International Atomic Energy Agency (IAEA), Vienna, Austria.

Marquardt ED, JP Le and R Radebaugh. 2002. "Cryogenic Material Properties Database." In *Cryocoolers 11, 11th International Cryocooler Conference*, pp. 681-687. June 20-22, 2000, Keystone, Colorado. DOI 10.1007/0-306-47112-4_84. Springer US.

NRC. 2002. *Recent Experience with Degradation of Reactor Pressure Vessel Head.* Information Notice 2002-11, U.S. Nuclear Regulatory Commission, Washington, D.C. March 12, 2002. U.S. NRC Agencywide Data Access and Management System (ADAMS) Accession Number ML020700556.

Appendix A

Precision EDM Notch Information

Appendix A

Precision EDM Notch Information

Precision square-edged electrical discharge machining (EDM) notches were an essential aspect of the CRDM nozzle mockup specimen. As described in the calibration specimen design section, a variety of notches were chosen for the mockup specimen and allowed for a multitude of ultrasonic calibrations to be made. Understanding the phased-array probe resolution and detection characteristics allowed for a more thorough leak-path assessment to occur on North Anna Unit 2 removed-from-service Nozzle 63.

This appendix highlights the exact as-built dimensions and locations for all notches used in the mockup assembly specimen as provided by Western Professional, Inc., the EDM notch subcontractor. Page A-2 lists the as-built dimensions for the 16 EDM notches placed in the carbon steel material representing the RPV head. Page A-3 lists the as-built dimension for the 16 EDM notches place in the outer diameter of the Alloy 600 tube. Page A-4 shows the requested placement and size of the notches on the Alloy 600 tube outer diameter. Page A-5 shows the requested placement and size of notches 9–12. Page A-6 shows the requested placement and size of notches 13–16. Page A-7 shows the requested notch layout and sizing for the carbon steel material inner diameter.

WESTERN PROFESSIONAL, INC.
DBA WESTPRO LAB
3460 BRADY COURT NE
SALEM, OR 97303
(503)585-6263

Electrical Discharge Machining
Reference Standard Manufacturing
Optical Dimensioning System
Non Destructive Evaluation
RT, UT, MT, PT

CUSTOMER:	BATTELLE	**STANDARD:**	BLOCK STANDARD **S/N 5381**
DRAWING #:	CUSTOMER DRAWING	**P.O. #:**	135771
MATERIAL:	CARBON STEEL	**SIZE:**	4.102" Ø HOLE
DATE:	11-11-10	**SPEC(S):**	PER CUSTOMER DRAWING INSTRUCTIONS

BLOCK STANDARD S/N 5381

DEFECT DIMENSIONS (IN INCHES)					
NO.	DEPTH	LENGTH	WIDTH	LOCATION	ORIENTATION
1	.0011"	2.0017"	.0364"	I.D.	LONGITUDINAL
2	.0020"	2.0048"	.0379"	I.D.	LONGITUDINAL
3	.0029"	1.9974"	.0377"	I.D.	LONGITUDINAL
4	.0049"	2.0046"	.0372"	I.D.	LONGITUDINAL
5	.1000"	1.9891"	.0316"	I.D.	LONGITUDINAL
6	.1004"	1.9929"	.0624"	I.D.	LONGITUDINAL
7	.1007"	2.0067"	.1251"	I.D.	LONGITUDINAL
8	.1002"	1.9968"	.2514"	I.D.	LONGITUDINAL
9	.0786"	1.0061"	.0833"	I.D.	TRANSVERSE
10	.0789"	1.0011"	.0826"	I.D.	TRANSVERSE
11	.0768"	1.0015"	.0834"	I.D.	TRANSVERSE
12	.0811"	1.0004"	.0827"	I.D.	TRANSVERSE
13	.0811"	1.0009"	.0807"	I.D.	LONGITUDINAL
14	.0789"	1.0028"	.0821"	I.D.	LONGITUDINAL
15	.0805"	1.0011"	.0828"	I.D.	LONGITUDINAL
16	.0805"	1.0007"	.0810"	I.D.	LONGITUDINAL

SEE ATTACHED DRAWING FOR NOTCH LOCATIONS

NOTE: ALL DEPTH AND WIDTH MEASUREMENTS ARE BASED ON AN AVERAGE OF FOUR OR MORE READINGS.

ALL DIMENSIONS ARE MEASURED WITH DIMENSIONAL EQUIPMENT WHICH IS CERTIFIED AND TRACEABLE TO NIST #(708) #2343033 AND NIST (#783183) #3881145. NUCLEAR REGULATORY COMMISSION RULES AND REGULATIONS 10 CFR PART 21 APPLIES TO THIS ORDER. ALL NOTCHES MANUFACTURED PER WESTPRO PROCEDURE WQC-IV.

CERTIFIED BY: S. CHAMBERLAIN

APPROVED BY: S. Chamberlain

WESTERN PROFESSIONAL, INC.
DBA WESTPRO LAB
3460 BRADY COURT NE
SALEM, OR 97303
(503)585-6263

Electrical Discharge Machining
Reference Standard Manufacturing
Optical Dimensioning System
Non Destructive Evaluation
RT, UT, MT, PT

CUSTOMER:	BATTELLE	**STANDARD:**	PIPE STANDARD S/N 5382
DRAWING #:	CUSTOMER DRAWING	**P.O. #:**	135771
MATERIAL:	STAINLESS STEEL, HT# L215S	**SIZE:**	4.112" Ø X .6837" AWT
DATE:	11-11-10	**SPEC(S):**	PER CUSTOMER DRAWING INSTRUCTIONS

PIPE STANDARD S/N 5382

DEFECT DIMENSIONS (IN INCHES)					
NO.	DEPTH	LENGTH	WIDTH	LOCATION	ORIENTATION
1	.0011"	1.9976"	.0367"	O.D.	LONGITUDINAL
2	.0020"	1.9951"	.0366"	O.D.	LONGITUDINAL
3	.0030"	1.9971"	.0370"	O.D.	LONGITUDINAL
4	.0050"	1.9994"	.0371"	O.D.	LONGITUDINAL
5	.0980"	1.9945"	.0314"	O.D.	LONGITUDINAL
6	.1002"	2.0004"	.0632"	O.D.	LONGITUDINAL
7	.1012"	2.0066"	.1274"	O.D.	LONGITUDINAL
8	.1009"	1.9971"	.2526"	O.D.	LONGITUDINAL
9	.0795"	1.0007"	.0826"	O.D.	TRANSVERSE
10*	.0797"	1.0000"	.0851"	O.D.	TRANSVERSE
11	.0806"	1.0018"	.0807"	O.D.	TRANSVERSE
12	.0806"	1.0007"	.0822"	O.D.	TRANSVERSE
13	.0804"	1.0004"	.0818"	O.D.	LONGITUDINAL
14	.0840"	1.0015"	.0816"	O.D.	LONGITUDINAL
15	.0780"	1.0020"	.0818"	O.D.	LONGITUDINAL
16	.0809"	1.0012"	.0829"	O.D.	LONGITUDINAL

SEE ATTACHED DRAWING FOR NOTCH LOCATIONS

*NOTCH #10 WIDTH IS .001" OVER MAXIMUM TOLERANCE.

NOTE: ALL DEPTH AND WIDTH MEASUREMENTS ARE BASED ON AN AVERAGE OF FOUR OR MORE READINGS.

ALL DIMENSIONS ARE MEASURED WITH DIMENSIONAL EQUIPMENT WHICH IS CERTIFIED AND TRACEABLE TO NIST #(708) #2343033 AND NIST (#783183) #3881145. NUCLEAR REGULATORY COMMISSION RULES AND REGULATIONS 10 CFR PART 21 APPLIES TO THIS ORDER. ALL NOTCHES MANUFACTURED PER WESTPRO PROCEDURE WQC-IV.

CERTIFIED BY: S. CHAMBERLAIN

APPROVED BY: S. Chamberlain

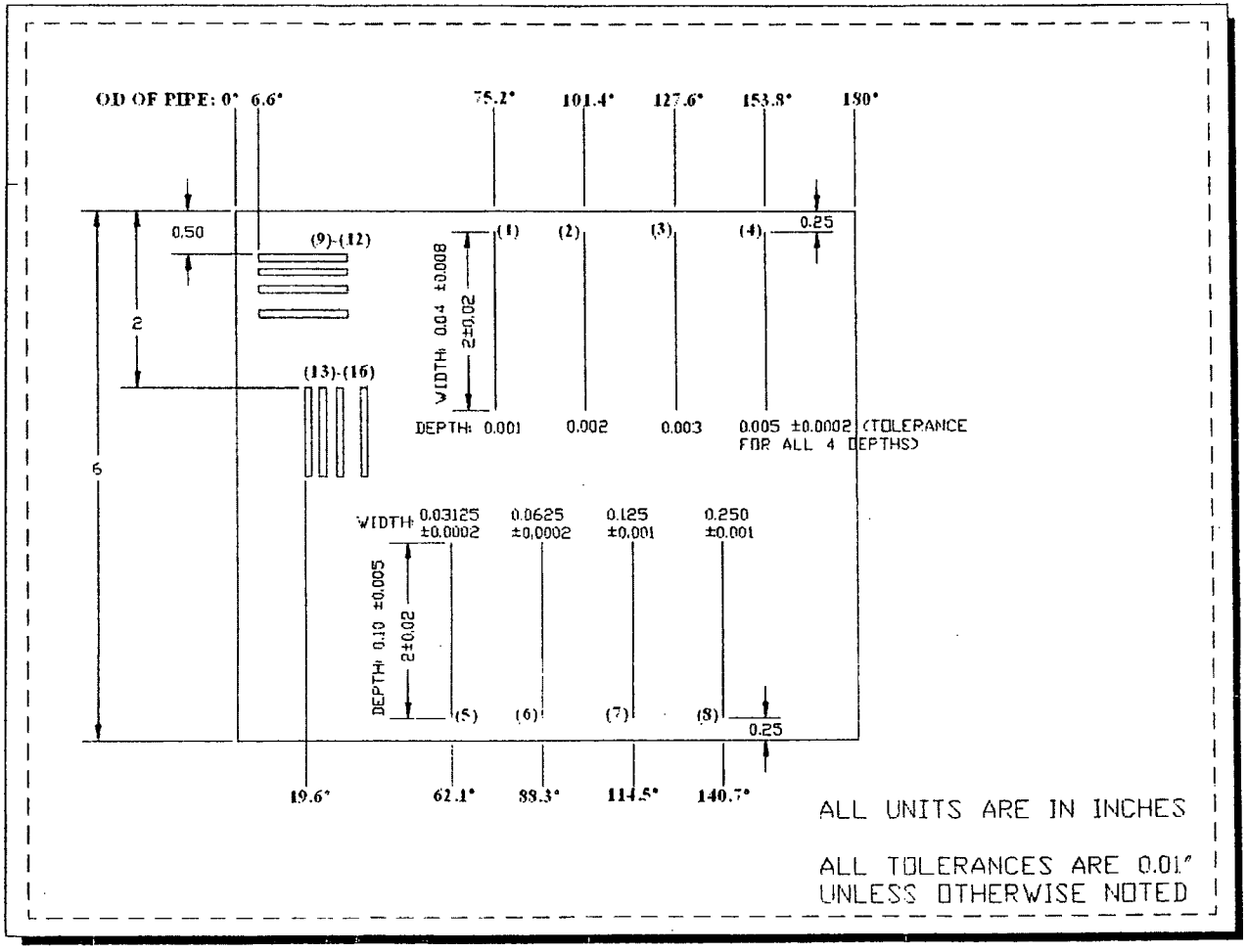
OD OF PIPE: 0° 6.6° 75.2° 101.4° 127.6° 153.8° 180°
0.50
(9)-(12)
2
(13)-(16)
6
WIDTH: 0.04 ±0.008
2±0.02
(1) (2) (3) (4)
0.25
DEPTH: 0.001 0.002 0.003 0.005 ±0.0002 (TOLERANCE FOR ALL 4 DEPTHS)
WIDTH: 0.03125 ±0.0002 0.0625 ±0.0002 0.125 ±0.001 0.250 ±0.001
DEPTH: 0.10 ±0.005
2±0.02
(5) (6) (7) (8)
0.25
19.6° 62.1° 89.3° 114.5° 140.7°
ALL UNITS ARE IN INCHES
ALL TOLERANCES ARE 0.01" UNLESS OTHERWISE NOTED

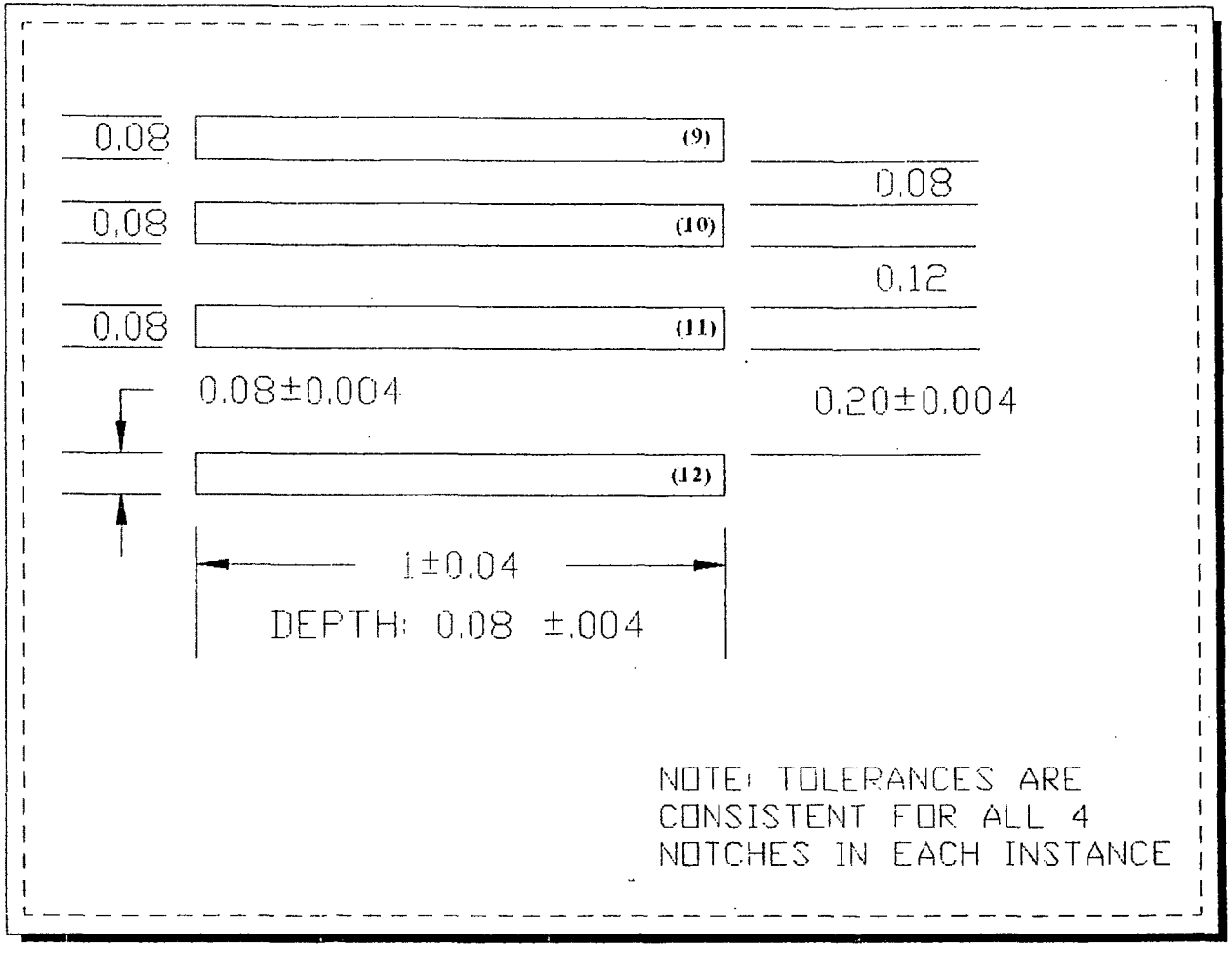
0.08
(9)
0.08
0.08
(10)
0.12
0.08
(11)
0.08±0.004
0.20±0.004
(12)
1±0.04
DEPTH: 0.08 ±.004
NOTE: TOLERANCES ARE CONSISTENT FOR ALL 4 NOTCHES IN EACH INSTANCE

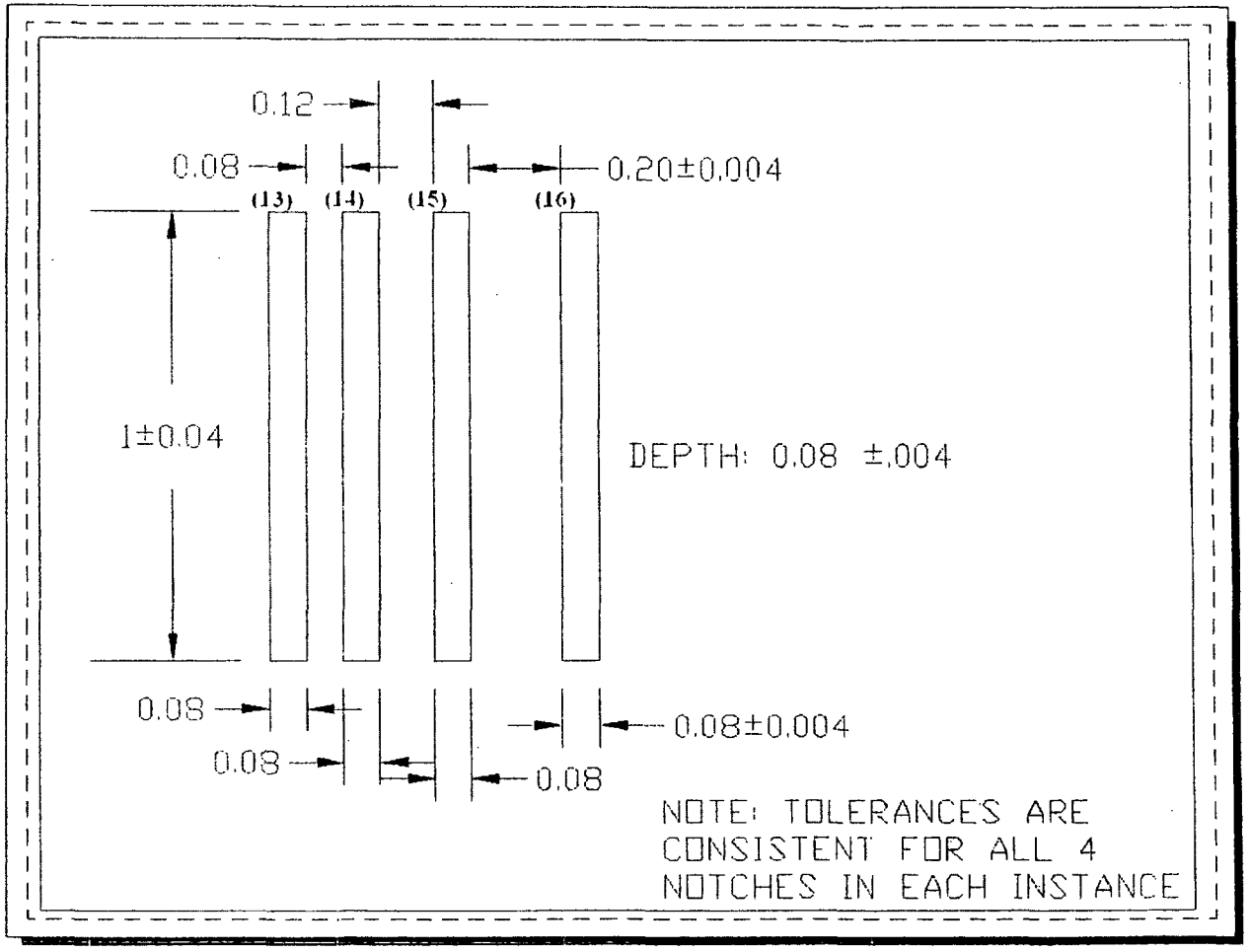
0.12
0.08
0.20±0.004
(13)
(14)
(15)
(16)
1±0.04
DEPTH: 0.08 ±.004
0.08
0.08
0.08
0.08±0.004
NOTE: TOLERANCES ARE CONSISTENT FOR ALL 4 NOTCHES IN EACH INSTANCE

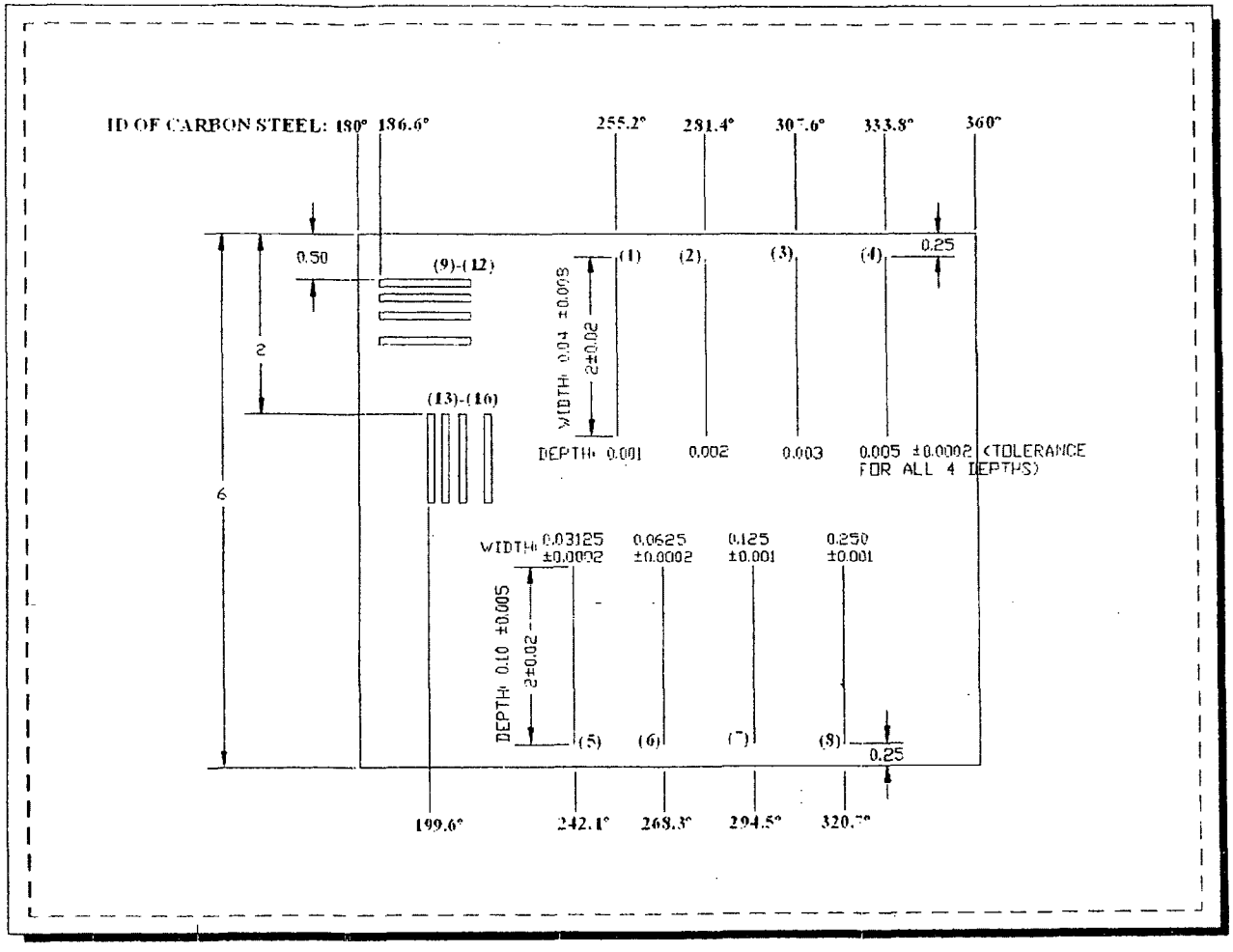
ID OF CARBON STEEL: 180° 186.6°
255.2°
281.4°
307.6°
333.8°
360°
0.50
(9)-(12)
2
(13)-(16)
6
(1)
(2)
(3)
(4)
0.25
WIDTH 0.04 ±0.005
2±0.02
DEPTH 0.001
0.002
0.003
0.005 ±0.0002 (TOLERANCE FOR ALL 4 DEPTHS)
WIDTH 0.03125 ±0.0002
0.0625 ±0.0002
0.125 ±0.001
0.250 ±0.001
DEPTH 0.10 ±0.005
2±0.02
(5)
(6)
(7)
(8)
0.25
199.6°
242.1°
268.3°
294.5°
320.7°